POLITECNICO DI TORINO
Repository ISTITUZIONALE

Go-or-grow models in biology: a monster on a leash

Original
Go-or-grow models in biology: a monster on a leash / Thiessen, R., Conte, M., Stepien, T.L., Hillen, T.. - In: JOURNAL OF MATHEMATICAL BIOLOGY. - ISSN 0303-6812. - 91:5(2025), pp. 1-45. [10.1007/s00285-025-02243-8]

Availability:
This version is available at: 11583/3004409 since: 2025-10-24T06:12:12Z

Publisher:
Springer

Published
DOI:10.1007/s00285-025-02243-8

Terms of use:

This article is made available under terms and conditions as specified in the corresponding bibliographic description in the repository

Publisher copyright

(Article begins on next page)

26 November 2026

J. Math. Biol. (2025) 91:58
https://doi.org/10.1007/s00285-025-02243-8

Mathematical Biology

Go-or-grow models in biology: a monster on a leash

Ryan Thiessen[1] · Martina Conte[2] · Tracy L. Stepien[3] · Thomas Hillen[1]

Received: 6 December 2024 / Revised: 3 April 2025 / Accepted: 25 May 2025
© The Author(s) 2025

Abstract
Go-or-grow approaches represent a specific class of mathematical models used to describe populations where individuals either migrate or reproduce, but not both simultaneously. These models have a wide range of applications in biology and medicine, chiefly among those the modeling of brain cancer spread. The analysis of go-or-grow models has inspired new mathematics, and it is the purpose of this review to highlight interesting and challenging mathematical properties of reaction–diffusion models of the go-or-grow type. We provide a detailed review of biological and medical applications before focusing on key results concerning solution existence and uniqueness, pattern formation, critical domain size problems, and traveling waves. We present new results related to the critical domain size and traveling wave problems, and we connect these findings to the existing literature. Moreover, we demonstrate the high level of instability inherent in go-or-grow models. We argue that there is currently no accurate numerical solver for these models, and emphasize that special care must be taken when dealing with the "monster on a leash".

Keywords Go-or-grow dichotomy · Glioma · Traveling Waves · Instabilities and Patterns · Critical domain size

Mathematical Classification 92B05 · 35B36 · 35M30

Ryan Thiessen and Martina Conte have contributed equally to the work.

✉ Martina Conte
conte.martina.93@gmail.com

[1] Department of Mathematical and Statistical Sciences, University of Alberta, Edmonton, Canada

[2] Department of Mathematical, Physical, and Computer Sciences, University of Parma, Parma, Italy

[3] Department of Mathematics, University of Florida, Gainesville, FL, USA

Published online: 16 October 2025

1 Introduction

Various biological processes involve a dichotomy between proliferation and migration: individuals in a population either remain relatively stationary and reproduce, or they migrate with minimal reproduction. This phenomenon has been particularly emphasized in the study of glioma progression, where the "go-or-grow" hypothesis was coined to describe the behavior of brain tumor cells (Hatzikirou et al. 2012).

The seminal work by Murray (2003) laid the groundwork for much of the existing mathematical modeling of glioma spread, which is based on the classical Fisher–Kolmogorov–Petrovsky–Piskounov (FKPP) equation. This reaction–diffusion macroscopic mathematical framework has been termed as the proliferation–infiltration (PI) model, as it captures both the proliferative and invasive behaviors of glioma cells observed in experiments and clinical settings. The strength of the PI model lies in its simplicity, requiring only a small set of parameters, which facilitates its calibration to patient-specific data. Extensions of the PI model account for the influence of surrounding tissue, chemical signals, and/or vasculature on glioma cell density (Swanson et al. 2003; Jbabdi 2005; Saut et al. 2014; Hormuth 2022; Swanson et al. 2008; Swanson 2011; Conte et al. 2021; Curtin 2020; Curtin et al. 2020). Advection bias in response to environmental cues has also been incorporated, either directly in the macroscopic model, based on mass/flux/momentum balance (Colombo 2015; Kim et al. 2009), or through more detailed descriptions derived from lower-scale dynamics, as initially proposed in Painter and Hillen (2013) and further developed in Conte et al. (2020); Engwer et al. (2015); Conte and Surulescu (2021); Engwer et al. (2016, 2015); Swan et al. (2018); Conte et al. (2023). Many models have also been developed in (semi)discrete settings (Böttger et al. 2012; Hatzikirou et al. 2012; Kim and Roh 2013). However, due to the complexity of glioma growth—spanning interactions between glioma cells, their microenvironment, immune cells, vasculature, and molecular signalling systems, all within the heterogeneous landscape of brain tissue—an exhaustive model remains elusive. As a result, models typically focus on well-defined subprocesses. Among these, the phenotypic heterogeneity of glioma cells plays a central role. While there are numerous reviews of mathematical modeling of gliomas (Hatzikirou et al. 2005; Martirosyan 2015; Alfonso 2017; Jørgensen 2023), this paper specifically focuses on a family of reaction–diffusion models of the go-or-grow type. In these models, a distinct separation between proliferating and migrating cells leads to systems of two coupled reaction–diffusion equations.

We will focus our attention on a go-or-grow model consisting of two coupled differential equations for the evolution of a moving subpopulation and a resting and proliferating subpopulation of cells. We assume linear diffusion for the moving population and neglect any small diffusivity in the resting population. Concerning the transition functions between the two subpopulations, we account for a general dependence on both subpopulation densities, defining this setting as the *general go-or-grow model*. As described above, there are several extensions of this framework that may include nonlinear diffusion of the moving compartment, general waiting time distributions, small diffusivity in the stationary compartment, or more complex population dynamics. Their analysis is rich, well-developed, and their analytical proper-

ties are vast (Murray 2003; Fedotov and Iomin 2008; Smoller 1983; Britton 1986; Kuznetsov and Kolobov 2020).

1.1 Paper outline

We first provide in Sect. 2 a detailed overview of the use of go-or-grow models for describing glioma dynamics (Sect. 2.1), reviewing the biological evidence of the go-or-grow dichotomy in glioma (Sect. 2.1.1) and the mathematical literature of go-or-grow models formulated with discrete, continuous, deterministic and stochastic approaches (Sect. 2.2). We also discuss applications of the go-or-grow dichotomy in ecology and other biological settings (Sect. 2.3).

In Sect. 3, we first review the classical FKPP equation as a reference point for further modeling and analysis. We then introduce the main players of this review article, namely the *general go-or-grow model* and its simplifications, which we call the *total population go-or-grow model*, where the transition functions depend on the sum of the two subpopulation densities (Pham 2012; Stepien et al. 2018; Tursynkozha et al. 2023; Syga et al. 2024; Böttger 2015; Falcó et al. 2024; Hatzikirou et al. 2012), and the *balanced go-or-grow model* and *constant rates go-or-grow model*, which fit into the context analyzed in (Gerlee and Nelander 2012, 2016; Fedotov and Iomin 2008; Falcó et al. 2024; Böttger 2015; Pham 2012; Syga et al. 2024). We show that for fast transition rates, a FKPP-type model can be found as the leading order approximation.

After the models are defined, we focus on some mathematical properties. In Sect. 4, we review a method by Rothe (1984) to obtain a general local and global existence result. This does, however, not prevent strange behavior, as we show in Sect. 5. Here we employ methods that were developed by Marciniak-Czochra (2015); Härting and Marciniak-Czochra (2014), to find that high-frequency instabilities are possible, and in fact, likely to occur. Section 6 focuses on the classical ecological problem of a critical domain size, investigating what is the minimum size of a domain to support a go-or-grow population by reviewing previous results of Hadeler and Lewis (2002); Lewis and Schmitz (1996). Section 7 then focuses on the existence of invasion waves and the estimation of the invasion speeds. We review previous results by Hadeler and Lewis (2002); Pham (2012); Stepien et al. (2018), and Falcó et al. (2024), and put them into an extended general framework. For this, we employ the general theory of invasion fronts of cooperative systems to generate a new result that applies in our more general framework. This section closes with a comparison of the wave speeds of the go-or-grow models to the FKPP wave speed.

This paper is rounded off with a discussion (Sect. 8) of the relevance of these models to both biology and mathematics and the mathematical challenges that are still open. The biological applications are manifold, and the mathematical problems are interesting and challenging.

2 Biological background and previous mathematical models

2.1 Motivation: glioma dynamics

Gliomas are the most frequent type of primary brain tumors. They originate from glial cells in the central nervous system and account for 78% percent of malignant brain tumors, of which glioblastoma multiforme (GBM) is the most aggressive subtype. It is characterized by infiltrative spread and fast proliferation. These features make GBMs relentless and deadly brain cancers, claiming the lives of most patients within eighteen months of diagnosis, with only a small percentage surviving beyond five years (Ostrom 2014; Wick et al. 2018).

A significant challenge stems from the highly invasive nature of gliomas, characterized by diffuse borders and recurrence of the disease around or within the treated area (Hou et al. 2006). Glioma cells not only invade locally, navigating through the extracellular matrix (ECM), but also exploit structured pathways such as myelinated fibers, vasculature, and white matter tracts, enabling them to travel great distances (Cuddapah et al. 2014; Hormuth 2022; Saut et al. 2014; Osswald 2015; Swan et al. 2018; Engwer et al. 2015). This results in GBMs often presenting with a heterogeneous and anisotropic shape.

2.1.1 Biological evidence of go-or-grow dichotomy in glioma

Many experiments with cultures of glioma cells suggest mutual exclusion of migratory and proliferative behavior, a mechanism known as the go-or-grow dichotomy (Godlewski et al. 2010; Giese et al. 2003; Xie et al. 2014; Berens and Giese 1999; Giese 1996; Wang 2012; Farin 2006), schematized in Fig. 1. Precisely, in Giese et al. (2003); Giese (1996) experimental evidence suggests that there may be an inherent and inverse correlation between cell motility and proliferation within a malignant glioma cell population, i.e., highly migratory glioma cells have a lower proliferation rate compared to those cells with weak migratory ability that proliferate much more. In Godlewski et al. (2010), a glioma-expressed microRNA that regulates the balance of proliferation and migration in response to metabolic stress is identified, revealing that, in addition to inhibiting glioma cell migration, this microRNA expression also

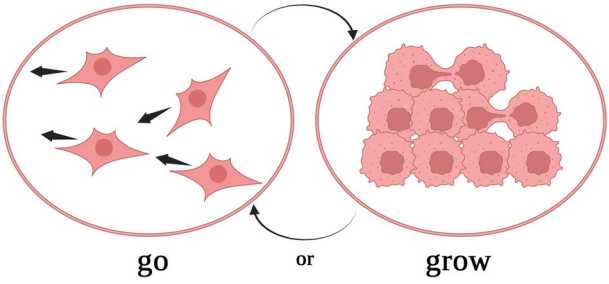


Fig. 1 Sketch of the go-or grow dichotomy. In this framework, cells can switch between a moving phenotype and a stationary and reproducing phenotype. Created in BioRender. Conte, M. (2024) https://biorender.com/i82o612

promotes cell proliferation. The role of the receptor tyrosine kinase EphB2 in controlling the proliferation/migration dichotomy in GBMs and its pro-invasive and anti-proliferative effects is later shown in Wang (2012). In Hoek (2008), the go-or-grow behavior is also observed in melanoma cells, although other studies suggest that the behavior appears to be specific to tumors of glial origin (Garay 2013).

However, the go-or-grow hypothesis does not apply to all tumor growth in general. For example, in Ratliff (2023); Odde (2023) the authors identified glioblastoma cells that exhibit both high proliferative and invasive capabilities simultaneously. In Ayuso (2017); Scribner and Fathallah-Shaykh (2017), the emergence of a go-and-grow phenotype under hypoxic conditions is observed. Similarly, in Vittadello et al. (2020) it is shown for melanoma that differentiating between solely moving or proliferating cancer cells could not be determined. Hence, the go-or-grow mechanism is not a universal phenomenon in cancer, although it has been reported in many cases and most prominently in glioma.

2.2 Mathematical approaches to the go-or-grow dichotomy in glioma

The large literature concerning mathematical models for the description of the go-or-growth mechanism in gliomas ranges from (semi)discrete to continuous approaches, from hybrid to stochastic methods. Moreover, within models of the same family, further classifications can be considered in relation to either the type of considered phenotypic switch functions (e.g. constant, density-dependent rates, or environmental-driven switching) or the characteristic of the operators modeling migration (e.g. linear or nonlinear diffusion, as well as additional tactic terms).

2.2.1 Stochastic and discrete models

One of the first publications investigating the go-or-grow mechanism is the model by Fedotov and Iomin (2008, 2007) that uses a continuous time random walk (CTRW) to formulate the balance equations for the cancer cells of two phenotypes with random switching between cell proliferation and migration. The CTRW describes tumor cell transport, assuming an arbitrary waiting time distribution between jumps and general jump kernels, while proliferation is modeled by logistic growth. The authors study the overall spreading rate, defined as the speed of the traveling wave solution of their system, and find its dependence on the statistical characteristics of the random switching process. From these first works, the literature on this topic started to expand.

A series of papers from Hatzikirou, Deutsch, and co-authors analyze the problem using lattice-gas cellular automaton (LGCA) models that account for unbiased cell random walk and cell proliferation influenced by the local oxygen concentration and according to a carrying capacity-limited mechanism. Phenotype changes either with constant probabilities (Böttger et al. 2012; Hatzikirou et al. 2012), local cell density-dependent rates (Böttger 2015; Tektonidis 2011; Syga et al. 2024), or in response to environmental stimuli (Kim and Roh 2013). The width of the invasive zone and the speed of the invasive front are analyzed in relation to the phenotypic transition parameter. In particular, in Böttger (2015); Syga et al. (2024) the authors

distinguish two scenarios depending on the parameter regions. In one case, called repulsive regime, the tumor cell population will inevitably grow. In the other case, called attractive regime, they identified conditions under which sufficiently small tumors die out. This is a phenomenon known as the Allee effect and it is deeply studied in ecology. Mean field approximations of the LGCA models are also provided, under the assumption that the switch dynamics are much faster than cell proliferation and death. The authors derive macroscopic descriptions of FKPP type, showing that there is a trade-off between diffusion and proliferation, reflecting the inability of cells to migrate and proliferate simultaneously.

With a methodology similar to Fedotov and Iomin (2008), in Gerlee and Nelander (2016, 2012) Gerlee and Nelander develop an individual-based (IB) stochastic model with constant switching rates between proliferating or migrating states. From it, they derive a system of macroscopic PDEs that establishes a connection between single cell characteristics and macroscopic behaviors. Precisely, their strategy is to formulate two coupled master equations for the occupation probabilities of the lattice sites and then approximate them by a set of PDEs. The derived macroscopic system features nonlinear diffusion for both cell populations, as well as additional transport for the moving cells, which makes the model different from the our minimal go-or-growth setting. Wave speed analysis is performed to show the influence of the parameters (switching, proliferation, motility, and apoptosis rate) on the wave speed. Moreover, under suitable simplified assumptions, a closed expression of the minimum wave speed is derived, as well as an approximate expression of the wavefront shape, using singular perturbation methods.

2.2.2 Continuous models

Inspired by the macroscopic counterparts of the above-described discrete approaches modeling the go-or-growth dichotomy in glioma cells, continuous formulations of such mechanism have been proposed. These approaches are either derived from multi-scale descriptions of cell dynamics or directly stated at the macroscopic level as reaction–diffusion models.

Concerning multi-scale models, Chauviere et al. (2010) build a model for two interacting cell populations with different migratory properties whose corresponding phenotype changes are induced by cell density effects. In particular, they investigate the phenotypic adaptation to dense and sparse environments, showing that when the cell migratory ability is reduced by a crowded environment, a diffusive instability may appear, leading to the formation of aggregates of cells of the same phenotype. Similar approaches to the same problem have been later proposed in a series of works accounting for the go-or-grow cell mechanism in response to constant or density-dependent rates (Engwer et al. 2015; Zhigun et al. 2018; Hillen et al. 2024; Alsisi et al. 2021) as well as different environmental factor, such as oxygen and nutrient availability, acidity (Conte and Surulescu 2021), therapy effects (Hunt and Surulescu 2017), or cell membrane receptors' concentration (Stinner et al. 2016). These approaches feature non-linear diffusion and transport terms for the moving cells. Moreover, in some of these works, results concerning the global existence of weak solutions for the derived macroscopic setting are proved (Stinner et al. 2016; Zhigun et al. 2018).

In this category, we also have to mention a recent work from Hillen and co-authors (Hillen et al. 2024), who propose a mathematical model for the microtube-induced glioma invasion in which, under suitable scaling arguments, a go-or-grow mechanism could be identified, *a posteriori*, justifying the earlier approaches. The idea of microtube-mediated cell invasion comes from some recent experiments (Osswald 2015) showing how glioma cells send out thin cell protrusions - the tumor microtubes - that form a network invading the healthy tissue, making connections between cells and enabling long-range cell-to-cell signaling.

Considering models directly stated at the macroscopic level in terms of reaction–diffusion systems of equations for the two cell sub-populations, a first approach can be found in Pham (2012). The described setting models a density-dependent go-or-grow mechanism, characterizing the development of spatio-temporal instabilities and traveling wave solutions. In the same context of density-dependent phenotypic changes, we must also account for the investigations collected in Stepien et al. (2018); Tursynkozha et al. (2023); Falcó et al. (2024). Precisely, in Stepien et al. (2018) the authors analyze the speed and shape of traveling wave solutions of a go-or-grow model for some specific expression of the phenotypic transition functions. They derive a closed form for the minimum wave speed and, adapting the method of Canosa (1973), obtain an approximation of the traveling wave solution. This study has then been then extended in Tursynkozha et al. (2023) for slightly more general phenotypic transition functions. Recently, in Falcó et al. (2024), a formal analysis of the traveling wave solutions has been presented in comparison with the classical results of the well-known FKPP equation. However, this has been obtained with simplified assumptions on the transition parameters, comparable with considering constant rate functions. Besides these studies, which relate to a minimal go-or-grow model similar to (4), it is worthy to mention some other works developed within the same biological context that, however, either account for small diffusion terms in the equation for the proliferative population (Burger et al. 2020; Pardo et al. 2016) or consider phenotypic transition rates depending on external signals (Alfonso 2016; Saut et al. 2014; Martınez-González et al. 2012; Stein et al. 2007, 2018; Crossley et al. 2024; Ayuso 2017). Models that incorporate the microenvironment include (Crossley et al. 2024) where the authors analyze a heterogeneous population comprising cells that can either move and degrade ECM or proliferate, including both nonlinear diffusion and an additional tactic term for the former, as well as the evolution of the ECM. They explore the impact of different switching mechanisms on the speed of the populations, including constant, ECM-dependent, and density-dependent switching rates.

2.3 Other applications

Go-or-grow models have also been used in ecological contexts for the description of immobile and dispersing populations and two-species competition settings. Studies of the “drift paradox”, where aquatic insects in streams with downstream drift are able to remain upstream, have included two-phase models where an insect is either mobile in the stream (moving with diffusion and advection) or stationary on the benthos (and reproducing), and insects transition between each phase (Pachepsky et al. 2005; Lutscher et al. 2006, 2007; Lutscher and Seo 2011; Huang et al. 2016; Liang

et al. 2017; Wang and Shi 2020; Yan et al. 2022). The benthic-drift model has also been extended to study the movement of zebra mussels in rivers (Huang et al. 2017; Jin and Zhao 2021). Some models of predator–prey systems or spreading of epidemics take on the form of two-equation reaction–diffusion systems with one population as the prey or the susceptible population and the other as the predator or the infected population, respectively (Capasso and Maddalena 1981; Dunbar 1983, 1984, 1986; Huang et al. 2003; Li and Wu 2008; Lin et al. 2011; Hsu et al. 2012; Huang 2012, 2016; Zhang et al. 2016; Zhao and Zhou 2016; Lam et al. 2018). Here, the populations only transition in one direction (from energy conversion from prey to predator or transfer from susceptible to infected population) and both may be mobile.

Other examples of go-or-grow mechanisms in biological modeling studies include movement of forest boundaries (Kuznetsov et al. 1994; Chuan et al. 2006), amoebae (Cochet-Escartin 2021), genetically engineered microbes (Lewis et al. 1996), cells during wound healing (Landman et al. 2007), genetic traits (Venegas-Ortiz et al. 2014), mRNA cargo (Ciocanel et al. 2018), and bacteria (Patra and Klumpp 2021).

Further afield, studies of autocatalytic chemical reactions often include reaction–diffusion equation systems with one-directional transitions and equal or differing diffusion constants for the reactant and autocatalyst (Billingham and Needham 1991; Merkin and Sadiq 1996; Merkin et al. 1996; Sadiq and Merkin 1996; Finlayson and Merkin 1997; Xin 2000). The reaction terms in the autocatalytic models inspired the form of the Klausmeier–Gray–Scott model, which examines stripe and pattern formation of vegetation depending on water movement (Van der Stelt et al. 2013; Sewalt and Doelman 2017; Chen and Wang 2024).

3 The go-or-grow model

In this section, we first introduce the classical FKPP equation (Murray 2002; Levin and Okubo 2002; Britton 1986), for which there is a vast developed literature and because it forms the basis for analysis of go-or-grow models due to their similar structure. Various go-or-grow models are subsequently stated, and the connection between the FKPP equation and go-or-grow models is demonstrated in the last subsection via the fast transition rate scaling.

3.1 FKPP equation

Letting $m(t,x)$ denote the population size at time $t \geq 0$ and spatial position $x \in \Omega \subset \mathbb{R}^k$, $k \geq 1$, then the FKPP reaction–diffusion equation reads

$$m_t = d\Delta m + f(m), \tag{1}$$

where the subscript t denotes the partial time derivative and Δ denotes the spatial Laplacian on Ω. Typically, $f(m)$ is of *logistic type*, i.e., it satisfies the following properties

$$f(0) = 0, \quad f(K) = 0, \quad f'(0) > 0, \quad f'(K) < 0, \quad \text{and} \quad f(m) > 0 \text{ for } 0 < m < K, \tag{2}$$

where $K > 0$ denotes the carrying capacity. In addition, we will often consider the *subtangential condition*, which is

$$f'(0)m \geq f(m), \qquad \text{for } \; 0 \leq m \leq K. \tag{3}$$

In the following, we will use the notation $f(m) = g(m)m$, where $g(m)$ denotes the per-capita growth rate of the population $m(t, x)$.

3.2 Go-or-grow model types

Go-or-grow models can be seen as a generalization of the FKPP equation. We first define the general continuous go-or-grow model that represents the focus of this review, and then several special variations that are used to address some of the mathematical challenges described in the subsequent sections.

General go-or-grow model. Let $u(t, x)$ denote the density of migrating cells and $v(t, x)$ the density of stationary and proliferating cells. The *general go-or-grow model* is the system of equations

$$\begin{cases} u_t = d\Delta u - \mu u - \alpha(u, v)u + \beta(u, v)v, \\ v_t = g(u + v)v + \alpha(u, v)u - \beta(u, v)v, \end{cases} \tag{4}$$

where $d > 0$ is a constant diffusion coefficient, $\mu \geq 0$ is a natural death rate for the moving compartment, $\alpha(u, v)$ denotes the transition rate function from the moving cell compartment to the stationary one, and $\beta(u, v)$ denotes the transition rate function from the stationary cell compartment to the moving one. The function $g(u + v)v$ accounts for the proliferation of the cell population, and, in the literature, it often takes a logistic form.

Total population go-or-grow model. Starting from the general model (4), a first variation of it is obtained by assuming that the transition rates α and β depend on the sum of the two populations, i.e., $\alpha = \alpha(n)$ and $\beta = \beta(n)$, with

$$n(t, x) = u(t, x) + v(t, x). \tag{5}$$

This version of the go-or-grow model has been used in many papers (e.g. Pham 2012; Falcó et al. 2024; Syga et al. 2024; Tektonidis 2011; Tursynkozha et al. 2023). We refer to it as the *total population go-or-grow model*, whose equations are given by

$$\begin{cases} u_t = d\Delta u - \mu u - \alpha(n)u + \beta(n)v, \\ v_t = g(n)v + \alpha(n)u - \beta(n)v. \end{cases} \tag{6}$$

Balanced go-or-grow model. If we consider that the transition probabilities from moving to stationary compartment and from stationary to moving compartment are balanced in the total population model (6), i.e., $\alpha(n) + \beta(n) = \gamma$, we obtain the *bal-*

anced go-or-grow model. Used in several works (e.g. Pham 2012; Böttger 2015); Syga et al. 2024), its equations read

$$\begin{cases} u_t = d\Delta u - \mu u + \gamma[\Gamma(n)v - (1-\Gamma(n))u], \\ v_t = g(n)v - \gamma[\Gamma(n)v - (1-\Gamma(n))u], \end{cases} \tag{7}$$

where $\gamma > 0$ denotes the rate at which a switch happens and $\Gamma(n)$ and $(1-\Gamma(n))$ are the probabilities that the switch is from moving to stationary compartment or vice versa, respectively.

Constant rates go-or-grow model. A further simplification of the previous models can be considered by assuming that the transition rates are constant, such as in Lewis and Schmitz (1996); Gerlee and Nelander (2016); Fedotov and Iomin (2008). We refer to this model as the *constant rates go-or-grow model*, which reads

$$\begin{cases} u_t = d\Delta u - \mu u - \alpha u + \beta v, \\ v_t = g(u+v)v + \alpha u - \beta v. \end{cases} \tag{8}$$

The constant rates model (8) may be seen as a special case of the balanced model (7) by setting

$$\gamma = \alpha + \beta \quad \text{and} \quad \Gamma = \frac{\beta}{\alpha+\beta}. \tag{9}$$

Analogously, the balanced model (7) may be seen a special case of the total population model (6) using the same assumption (9) and considering the rate γ depending on the total population.

For later use, it is useful to write the above models in vector form as

$$\mathbf{w}_t = D\Delta\mathbf{w} + \mathbf{F}(\mathbf{w}), \tag{10}$$

where $\mathbf{w} = (u, v)^T$, $D = \mathrm{diag}(d, 0)$, and

$$\mathbf{F}(\mathbf{w}) = \begin{pmatrix} -\mu u - \alpha(u,v)u + \beta(u,v)v \\ g(u+v)v + \alpha(u,v)u - \beta(u,v)v \end{pmatrix}. \tag{11}$$

In this formulation, (10) clearly resembles (1).

3.3 Fast transition rate scaling

We begin by reviewing a well-known scaling technique used to connect the mathematical properties of the go-or-grow type of models with the classical FKPP Eq. (1). The *fast transition rate scaling* is based on the natural assumption that the transitions between stationary and moving states are fast as compared to proliferation and diffu-

sion. Letting $\varepsilon > 0$ be a small parameter, we consider the general go-or-grow model (4) with fast transition rates $\alpha \sim \alpha/\varepsilon$ and $\beta \sim \beta/\varepsilon$, resulting in

$$\begin{cases} u_t = d\Delta u - \mu u - \dfrac{1}{\varepsilon}\left(\alpha(u,v)u - \beta(u,v)v\right), \\ v_t = g(u+v)v + \dfrac{1}{\varepsilon}\left(\alpha(u,v)u - \beta(u,v)v\right). \end{cases} \tag{12}$$

We introduce the regular perturbation expansion of $u(t,x)$ and $v(t,x)$,

$$u(x,t;\varepsilon) = u_0(t,x) + \sum_{n=1}^{\infty} u_n(t,x)\varepsilon^n,$$
$$v(x,t;\varepsilon) = v_0(t,x) + \sum_{n=1}^{\infty} v_n(t,x)\varepsilon^n,$$

and we assume that α, β, and g are of order $O(1)$ and sufficiently smooth to allow for a Taylor expansion about (u_0, v_0). Further assuming that each order of ε-terms vanishes independently, the zeroth order of ε reads

$$-\alpha(u_0,v_0)u_0 + \beta(u_0,v_0)v_0 = 0\,, \tag{13}$$

while the first order of ε gives

$$\begin{aligned}(u_0)_t =& d\Delta u_0 - \mu u_0 - \alpha(u_0,v_0)u_1 + \beta(u_0,v_0)v_1 \\ &- (u_1,v_1)\cdot\nabla_{uv}\alpha(u_0,v_0)u_0 + (u_1,v_1)\cdot\nabla_{uv}\beta(u_0,v_0)v_0,\end{aligned} \tag{14}$$

$$\begin{aligned}(v_0)_t =& g(u_0+v_0)v_0 + \alpha(u_0,v_0)u_1 - \beta(u_0,v_0)v_1 \\ &+ (u_1,v_1)\cdot\nabla_{uv}\alpha(u_0,v_0)u_0 - (u_1,v_1)\cdot\nabla_{uv}\beta(u_0,v_0)v_0,\end{aligned} \tag{15}$$

where ∇_{uv} is used to distinguish the derivatives with respect to u and v from the spatial derivatives. Summing (14) and (15), and then together with (13), we get the system

$$\begin{cases} (u_0+v_0)_t = (d\Delta - \mu)u_0 + g(u_0+v_0)v_0, \\ -\alpha(u_0,v_0)u_0 + \beta(u_0,v_0)v_0 = 0. \end{cases} \tag{16}$$

The second equation in (16) is an implicit equation for u_0 and v_0. We can use the implicit function theorem to find v_0 as a function of u_0 if

$$\frac{\partial\beta(u_0,v_0)}{\partial v_0}v_0 + \beta(u_0,v_0) - \frac{\partial\alpha(u_0,v_0)}{\partial v_0}u_0 \neq 0.$$

For particular forms of the transition rate functions α and β, it is possible to explicitly compute the inverse function.

The first example of using the fast-transition rate scaling in go-or-grow models appears in Hadeler and Lewis (2002) for the constant rates model (8). Under this model, it is possible to simplify system (16) to a single equation for the total population n, obtaining a convex combination of diffusion and growth as

$$n_t = \frac{\beta}{\alpha+\beta} d\Delta n + \frac{\alpha}{\alpha+\beta} g(n) - \frac{\mu\beta}{\alpha+\beta} n. \tag{17}$$

Here, the ratios $\beta/(\alpha+\beta)$ and $\alpha/(\alpha+\beta)$ represent the average fractions of the total cell population that belongs to the moving and stationary phase, respectively.

In the context of the total population go-or-grow model (6), an example of fast-transition rate scaling is done in Falcó et al. (2024) with $\mu = 0$ and $d = 1$. The following single governing equation in terms of the total population n is obtained:

$$n_t = \nabla \cdot (D(n)\nabla n) + \frac{\alpha(n)}{\alpha(n)+\beta(n)} n(1-n), \tag{18}$$

where the density-dependent diffusion takes the form

$$D(n) = \frac{\alpha(n)\beta'(n) - \alpha'(n)\beta(n)}{(\beta(n)+\alpha(n))^2} \frac{\beta(n)}{\beta(n)+\alpha(n)}. \tag{19}$$

The natural assumptions that $\alpha(n)$ is a non-increasing function of the total cell density and $\beta(n)$ is a non-decreasing function guarantee that $D(n) \geq 0$ for any $n \geq 0$. If α and β are constant, we return to Eq. (17), which is of FKPP type (1). Moreover, under the assumption that cells remain proliferative at low densities, i.e., $\beta(0) = 0$, a diffusion coefficient is obtained which resembles typical non-linear equations with degenerate diffusion.

Finally, in Scribner and Fathallah-Shaykh (2017), the authors compare a go-or-grow type model to a single-population model, showing how the single-population model replicate key features of glioblastoma progression. While their go-or-grow model includes switching functions based on factors other than cell density. It is important to note that the parameters used for comparison in the go-or-grow model (see Table 2 in Scribner and Fathallah-Shaykh (2017)) are an order of magnitude larger than the other rates. This scaling satisfies the assumption of the fast transition rate approximation, which helps explain why the simulation results from both models are similar.

4 A general existence result

All the models introduced in the previous section are based on the coupling of an ordinary differential equation with a reaction–diffusion equation. It is possible to prove a general existence result by using the existence theory for mixed type equations presented in Rothe (1984). Here, we recall the main assumptions and definition.

Let us consider system (4) in the form

$$\begin{cases} u_t = d\Delta u - du + (d-\mu)u - \alpha(u,v)u + \beta(u,v)v, \\ v_t = g(u+v)v + \alpha(u,v)u - \beta(u,v)v, \end{cases} \tag{20}$$

where we explicitly write the terms $-du + du$ so that $d(\Delta - 1)$ can be identified as a generator that has no eigenvalue equal to 0 in typical Neumann and periodic boundary conditions. In the case of Dirichlet boundary conditions, we do not need to use this trick and instead consider $d\Delta$ as the generator.

Definition 1 A *mild solution* (u, v) of (20) satisfies

$$(u,v) \in L^\infty([0,T)\times\Omega)^2,$$

$$u(\cdot,t) = S(t)u_0 + \int_0^t S(t-s)\Big((d-\mu)u(s) - \alpha(u(s),v(s))u(s) + \beta(u(s),v(s))v(s)\Big)ds,$$

$$v(\cdot,t) = v_0 + \int_0^t g(u(s)+v(s))v(s) + \alpha(u(s),v(s))u(s) - \beta(u(s),v(s))v(s)\, ds,$$

where $u(s) = u(\cdot, s)$ and $v(s) = v(\cdot, s)$, while $S(t)$ denotes the semigroup generated by $d(\Delta - 1)$ on $L^\infty(\Omega)$ with the boundary conditions (23) defined below.
Let us introduce the following set of assumptions.

- $\Omega \subset \mathbb{R}^k$ is a smooth bounded domain with Hölder continuous boundary, i.e.,

$$\Omega \in C^{2+\alpha}, \quad \alpha \in (0,1). \tag{21}$$

- The initial conditions satisfy

$$\bar{u}_0, \bar{v}_0 \in L^\infty(\Omega). \tag{22}$$

- There are differentiable functions $a(x) \geq 0$, $b(x) \geq 0$, $a(x)$ and $b(x)$ not simultaneously equal to 0, such that for all $x \in \partial\Omega$

$$b(x)u(t,x) + a(x)\frac{\partial}{\partial \hat{n}}u(t,x) = 0, \tag{23}$$

  where $\hat{n}$ denotes the outer normal vector on $\partial\Omega$.
- For each bounded set $B \in \mathbb{R}^2$ there exists a constant C_B such that for all

$(u, v), (w, y) \in B$

$$\begin{aligned} &|g(u+v) + \alpha(u,v) + \beta(u,v)| \leq C_B, \\ &|g(u) - g(w)| \leq C_B|u-w|, \\ &|\alpha(u,v) - \alpha(w,y)| \leq C_B(|u-w| + |v-y|), \\ &|\beta(u,v) - \beta(w,y)| \leq C_B(|u-w| + |v-y|). \end{aligned} \tag{24}$$

- The functions $g, \alpha, \beta \in C^2$; moreover,

$$\bar{u}_0 \in C^{2+\alpha}, \bar{v}_0 \in C^{\alpha} \tag{25}$$

and $\bar{u}_0$ satisfies the boundary conditions.

Theorem 1 *(Theorem 1 in Rothe (1984) (pages 111-112)) Assume (21)–(24), then (4) has a unique mild solution which is bounded in L^∞. If the maximal time of existence $T_{max} < \infty$, then*

$$\lim_{t \to T_{max}} \|(u(t,x), v(t,x))\|_\infty = \infty.$$

Moreover, if (25) holds, then for all $T < T_{max}$, the solutions are classical with

$$u \in C^{2+\alpha, 1+\alpha/2}(\bar{\Omega} \times [0,T)), \qquad v \in C^{\alpha, 1+\alpha/2}(\bar{\Omega} \times [0,T)).$$

Theorem 1 applies to all our variants of the go-or-grow models (4)–(8) with appropriate adjustments in the assumptions on the parameters. If a small diffusion term ($\epsilon \Delta v$) is considered in the equation for the proliferative population, e.g., as done in Burger et al. (2020), then standard semigroup methods can be applied to find solutions to the system (see Robinson 2001; Hillen 2023).

5 Instabilities and pattern formation

It is time to meet the monster on a leash. Marciniak-Czochra and collaborators have worked intensively on systems of reaction–diffusion equations coupled to ODEs Marciniak-Czochra (2015); Härting and Marciniak-Czochra (2014). In the study of Turing-like pattern formation, they made an interesting discovery, which is that all smooth patterns are unstable, and non-constant steady states need to have jumps. They also found that high frequencies are unstable in the linearization. This has far-reaching consequences, also for our study here, as we will outline in this section.

5.1 The general case

The ability of reaction–diffusion systems to form spatial patterns is a well researched area (Turing 1952; Murray 2003; Britton 1986; Levin and Okubo 2002). In a typical activator-inhibitor situation, for example, we consider a system of two reaction–dif-

fusion equations, where one species is the activator and the other the inhibitor. Turing patterns arise for a short range activator and a long range inhibitor (Turing 1952; Murray 2003; Britton 1986; Levin and Okubo 2002). The extreme situation would be a fully local activator, i.e., an activator without a diffusion term in the equations, leading to an ODE coupled to the PDE of the inhibitor. Hence, it is natural to expect that ODE-PDE systems can generate diffusion driven instabilities (Marciniak-Czochra 2015; Härting and Marciniak-Czochra 2014), and we review some of the results here.

For a coupled system of the form

$$\begin{cases} u_t = d_u \Delta u + k(u, v), \\ v_t = h(u, v), \end{cases} \tag{26}$$

on a smooth domain with standard boundary conditions, a necessary and sufficient condition for diffusion driven instability at a steady state $(\bar{u}, \bar{v})$ is the *autocatalysis condition*

$$\frac{\partial h}{\partial v}(\bar{u}, \bar{v}) > 0. \tag{27}$$

A proof is given in Theorem 4 in Marciniak-Czochra (2015), and we sketch some of the important steps here. If we abbreviate the partial derivatives at steady state as

$$k_u = k_u(\bar{u}, \bar{v}), \qquad k_v = k_v(\bar{u}, \bar{v}), \qquad h_u = h_u(\bar{u}, \bar{v}), \qquad h_v = h_v(\bar{u}, \bar{v}),$$

then the Jacobian of the kinetic part of (26) evaluated at $(\bar{u}, \bar{v})$, together with its trace and determinant is

$$A := \begin{pmatrix} k_u & k_v \\ h_u & h_v \end{pmatrix}, \qquad \mathrm{tr} A = k_u + h_v, \qquad \det A = k_u h_v - k_v h_u.$$

To study diffusion-driven instability, we assume that $(\bar{u}, \bar{v})$ is stable for the kinetic part, i.e.

$$\mathrm{tr} A < 0 \quad \text{and} \quad \det A > 0. \tag{28}$$

We linearize the full system (26) at the homogeneous steady state $(\bar{u}, \bar{v})$, and we use the Fourier transform with dual variable ω. The dual variable ω plays the role of the mode. For example, if we restrict on a given interval $[0, L]$, then we have only discrete modes $\omega_k = \frac{k\pi}{L}$ for $k \in \mathbb{N}$. The use of an abstract variable ω here allows us to make the following calculations as if ω were a continuous variable, while later, we can restrict to the discrete values ω_k. The Jacobian of (26) at $(\bar{u}, \bar{v})$ becomes

$$J = \begin{pmatrix} -d_u \omega^2 + k_u & k_v \\ h_u & h_v \end{pmatrix},$$

which has trace and determinant

$$\mathrm{tr}J = -d_u\omega^2 + \mathrm{tr}A < 0, \qquad \det J = -d_u\omega^2 h_v + \det A.$$

Hence we observe diffusion driven instability if $\det J < 0$, i.e.,

$$\omega^2 > \frac{\det A}{d_u h_v}. \tag{29}$$

Under this assumption, we find the corresponding eigenvalues of J as

$$\lambda_{1,2} = \frac{\mathrm{tr}A}{2} \pm \frac{1}{2}\sqrt{\mathrm{tr}J^2 - 4\det J},$$

where $\lambda_1 > 0$ and $\lambda_2 < 0$. It is interesting to look at the unstable eigenvalue λ_1 as a function of the mode ω,

$$\lambda_1(\omega) = \frac{1}{2}(-d_u\omega^2 h_v + \mathrm{tr}A) + \frac{1}{2}\sqrt{(-d_u\omega^2 h_v + \mathrm{tr}A)^2 - 4(-d_u\omega^2 h_v + \det A)}. \tag{30}$$

Using elementary calculations, we can show (skipping the details) that for

$$\omega = \bar{\omega} = \sqrt{\frac{\det A}{d_u h_v}},$$

we have $\lambda_1(\bar{\omega}) = 0$. Moreover, $\lambda_1(\omega)$ is strictly increasing for $\omega \geq \bar{\omega}$ and it goes into saturation

$$\lim_{\omega\to\infty} \lambda_1(\omega) = 2(2 - \mathrm{tr}A) > 0.$$

Hence, $\lambda_1(\omega)$ has the qualitative form shown in Fig. 2, which illustrates that higher modes are more unstable than smaller modes. This is the main reason why smooth non-constant steady states are unstable (Marciniak-Czochra 2015; Härting and Marciniak-Czochra 2014). Moreover, this observation also has direct consequences for

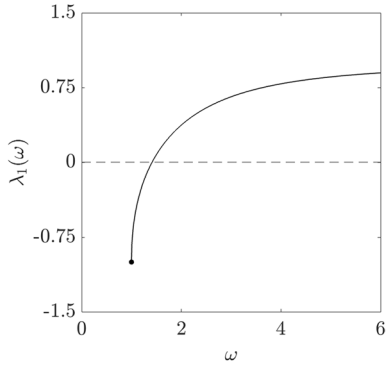


Fig. 2 Qualitative trend of $\lambda_1(\omega)$. Typical form of the unstable eigenvalue $\lambda_1(\omega)$ computed from (30) as function of the mode ω. Here, the parameters are set to $d_u = 1$, $k_u = -2$, $k_v = -2$, $h_v = 1$, and $h_u = 2$.

numerical computation. Note that different choices of parameters than those chosen in Fig. 2 give qualitatively the same form.

Now, we consider a discretization of our domain with a step size Δx. Then the spatial frequency is Δx^{-1}. According to what we just observed for $\lambda_1(\omega)$, each mode $\omega > \Delta x^{-1}$ is unstable. For example, using homogeneous Neumann boundary conditions on an interval $[0, L]$, then $\omega_k = k\pi/L$ and each mode k with $\omega_k > \Delta x^{-1}$ is unstable. Hence, in the Neumann case, and also in other cases, small errors on the scale of the numerical discretization are amplified, making the numerics unstable. Reducing the step size does not help, as then higher modes are still unstable. This appears to be a principal challenge of the ODE-PDE coupled systems, and in such a situation, an accurate numerical solver is inconceivable. In Fig. 3, we show a simulation of the balanced model (7) on a rectangular domain of size $[0, 50] \times [0, 50]$ for the transition and growth functions

$$\Gamma(n) = \frac{1}{2}\left(1 + \tanh[\nu(n^* - n)]\right), \qquad g(n) = r\left(1 - \frac{n}{K}\right). \tag{31}$$

In this case, the above conditions (27), (28), and (29) for diffusion-driven instability are satisfied. We simulate the system (7) by using the method of lines and discretizing

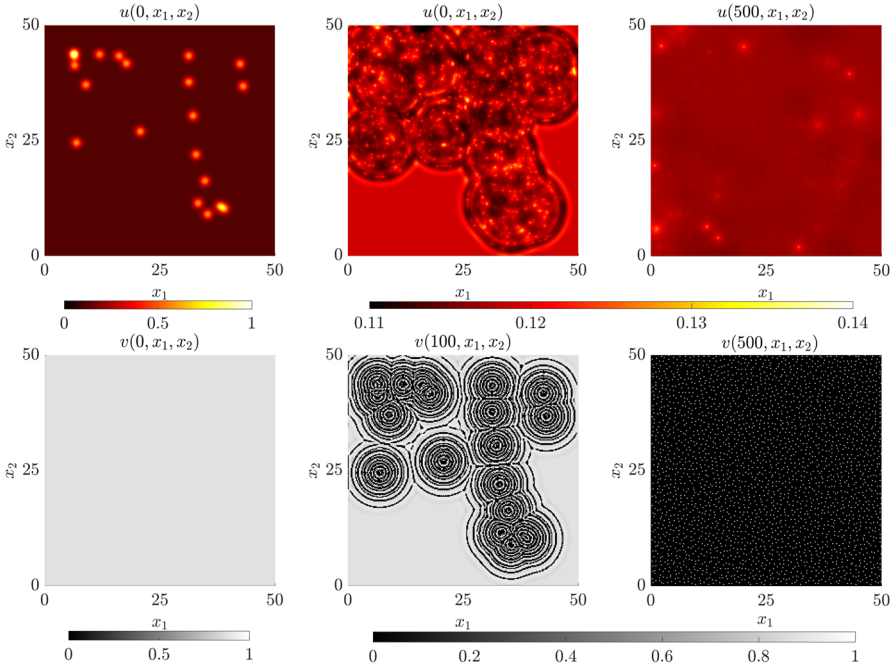


Fig. 3 Example of 2D instabilities emerging from model (7). Two-dimensional simulations of the balanced model (7) on a rectangular domain of size $[0, 50] \times [0, 50]$ for the transition and growth functions (31). The first row shows the evolution of the population $u(t, x)$, while the second row illustrates $v(t, x)$, with $x = (x_1, x_2)$. The three columns illustrate the population behavior at $t = 0, 100, 500$, respectively. The regular mesh size is set to $\Delta x_1 = \Delta x_2 = 0.2$, while the parameter values are chosen as $\nu = 4$, $K = 1$, $r = 1$, $\gamma = 1.6$, $n^* = 0.75$, and $d = 1$.

in space using a hybrid finite volume finite difference scheme, adapted from Thiessen and Hillen (2021). The solution converges to a smooth solution for u and a spatial pattern for v that is on the size of the discretization.

To further analyze the impact of the discretization, we illustrate in Fig. 4 the final state of the v variable when we reduce or enlarge Δx. We clearly see that the solution depends on the choice of Δx. We admit that normally, when a solution depends on the discretization, it implies that the numerical method is not good enough. But as we describe earlier, this is not due to an inappropriate numerical solver, rather, it is a systematic problem of this kind of models.

5.2 The go-or-grow case

Let us now employ the above results for go-or-grow models. Turing patterns for go-or-grow were previously considered by Pham (2012) for the balanced model (7). The function $g(n)$ is assumed to be non-increasing ($g' \leq 0$ with $g(1) = 0$). In this case, we have two homogeneous steady states, $(0, 0)$ and $(\Gamma(1), 1 - \Gamma(1))$. We assume that $(0, 0)$ is linearly unstable, such that a tumor can indeed grow, and consider diffusion driven instabilities at $(\Gamma(1), 1 - \Gamma(1))$. Checking the autocatalysis condition (27), a necessary and sufficient condition for diffusion driven instability is

$$\gamma(\Gamma(1) + \Gamma'(1)) - g'(1)(1 - \Gamma(1)) < 0. \tag{32}$$

This condition was derived by Pham (2012) for the special choice of $g(n) = 1 - n$. Note that since g is assumed to be non-increasing, an increasing probability function $\Gamma(n)$ can never satisfy (32). However, a decreasing function $\Gamma(n)$ with $|\Gamma'(n)|$ large enough can satisfy (32).

Performing a linear stability analysis of the balanced model (7), we find that under condition (32) all unstable modes ω satisfy (29), which in this context becomes

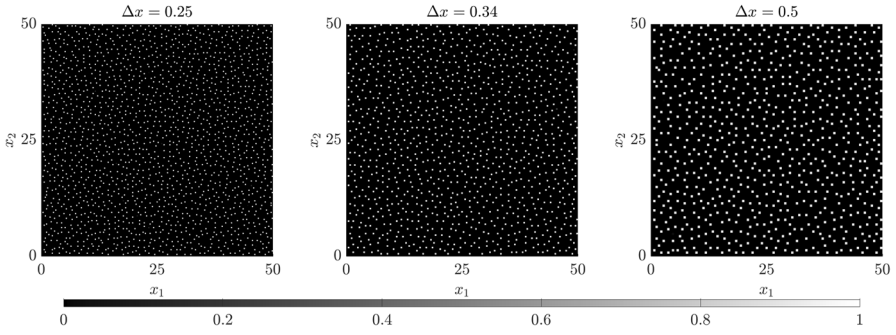


Fig. 4 Example of 2D instabilities emerging from model (7). Two-dimensional simulations at time $t = 500$ of the population $v(t, x)$ with $x = (x_1, x_2)$, for the balanced model (7) for three increasing value of the mesh size: $\Delta x = 0.25, 0.34, 0.5$. Here $\Delta x = \Delta x_i$, for $i = 1, 2$. The model is simulated on a rectangular domain of size $[0, 50] \times [0, 50]$ for the transition and growth functions (31). Parameters values are set to $\nu = 4$, $K = 1$, $r = 1$, $\gamma = 1.6$, $n^* = 0.75$, and $d = 1$.

$$\omega^2 > \frac{\gamma g'(1)(1-\Gamma(1))}{\gamma(\Gamma(1)+\Gamma'(1)) - g'(1)(1-\Gamma(1))}. \tag{33}$$

Note that we use again the mode ω as a continuous variable here. If we consider the balanced model (7) on an interval $[0, L]$ with homogeneous Neumann or Dirichlet boundary conditions, then the modes become $\omega_k = k\pi/L$.

For the probability of switching from stationary to moving (Pham 2012), there are two choices:

- *Attractive case:* $\Gamma(n)$ is a decreasing smooth step function connecting $\Gamma(n) \approx 1$ for small n to $\Gamma(n) \approx 0$ for large n. Specifically,

$$\Gamma(n) = \frac{1}{2}(1 + \tanh(\nu(n^* - n))),$$

  where n^* is the population size such that $\Gamma(n^*) = 0.5$. In this case, cells are more motile at low densities and more stationary at high densities.

- *Repulsive case:* $\Gamma(n)$ is an increasing smooth step function connecting $\Gamma(n) \approx 0$ for small n to $\Gamma(n) \approx 1$ for large n. Specifically,

$$\Gamma(n) = \frac{1}{2}(1 - \tanh(\nu(n^* - n))).$$

  Cells are more motile at high densities and less motile at low densities.

In the repulsive case, we have $\Gamma' > 0$ and condition (32) cannot be satisfied, but in the attractive case, we have $\Gamma' < 0$ and for sufficiently large ν, condition (32) can be satisfied. Pham (2012) show numerical simulations for the attractive case that leads to spatial pattern formation and irregular traveling waves. However, Pham (2012) do not discuss the high level of instability in their numerics. In Fig. 5, we show our own

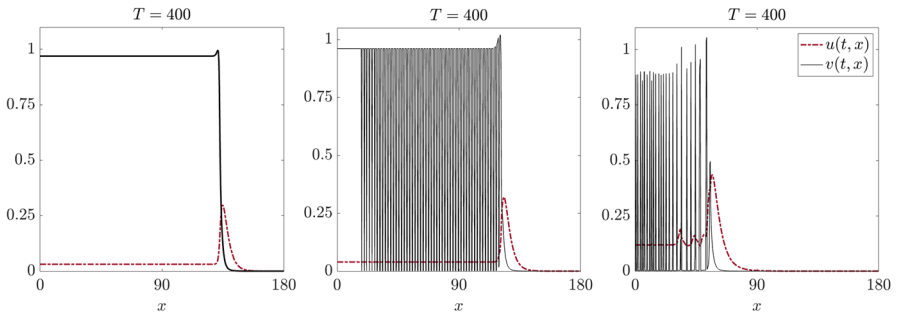


Fig. 5 Examples of 1D instabilities from model (7). One-dimensional simulations of the balanced model (7) on the domain [0, 180] for the transition and growth functions (31). The value of n^* is increased from left to right: $n^* = 0.57$, $n^* = 0.6$, and $n^* = 0.75$. The other parameters are set to $\nu = 4$, $K = 1$, $r = 1$, $\mu = 1.6$, and $d = 1$.

simulations of the traveling invasion waves of Pham (2012). As in Figs. 3 and 4, we observe instabilities behind the wave on the scale of the discretization. Hence, we can not ensure that the numerical solver is correct in those cases.

We have highlighted the rich array of intriguing mathematical properties related to the emergence of unusual behaviors and instabilities within the proposed framework. In the following, we focus on two well-established mathematical aspects for which more conclusive results can be obtained: the critical domain size problem and the traveling wave analysis.

6 Critical domain size

A common focus in spatial ecology is to identify the minimal size of a habitat such that a species has enough resources to survive, known as the critical domain size (de Vries et al. 2006; Murray 2003; Britton 1986; Levin and Okubo 2002). This has relevance in determining how large a habitat must be for species survival or how small it must be so that a parasite cannot establish itself.

6.1 The FKPP case

We first review the analysis of the critical domain size for the FKPP Eq. (1) under homogeneous Dirichlet boundary conditions. We look for nontrivial steady states, which are nonnegative solutions of the boundary value problem,

$$\begin{cases} -d\Delta m = g(m)m & \text{in } \Omega, \\ m = 0 & \text{on } \partial\Omega, \end{cases} \tag{34}$$

where $\Omega \in \mathbb{R}^d$ is a bounded domain with a smooth boundary $\partial\Omega$. We denote by $\lambda_1(\Omega)$ the value of the leading eigenvalue of $-\Delta$ on Ω. This eigenvalue often plays an important role in growth phenomena on a given domain, and it will be the determining value here. In particular, there is a bifurcation in the behavior of solutions of (34) based on the size of the principal eigenvalue and the growth rate of the population at zero, i.e., $g(0)$.

Theorem 2 *(Theorems 4.60−4.61 in Britton 1986) If the growth function $g \in C^2(\mathbb{R})$ is of logistic type (2), and satisfies the subtangential condition (3), then we have two cases:*

1. *If $\lambda_1(\Omega) \leq \dfrac{g(0)}{d}$, then (34) has a nontrivial solution;*
2. *If $\lambda_1(\Omega) > \dfrac{g(0)}{d}$, then (34) only has the trivial solution.*

This general result leads to the question of how the leading eigenvalue λ_1 depends on the domain size, which is clarified in the following theorem.

Theorem 3 *(Theorem 2.21 in Wang and Pang 2024) For the eigenvalue problem associated with $-\Delta$, $\lambda_1(\Omega)$ is strictly decreasing with respect to Ω, in the sense that if $\Omega \subset \tilde{\Omega}$, then $\lambda_1(\Omega) \geq \lambda_1(\tilde{\Omega})$, and $\Omega \subsetneq \tilde{\Omega}$ implies $\lambda_1(\Omega) > \lambda_1(\tilde{\Omega})$.*

The dependency on the domain size may furthermore be made more explicit by looking at the one-dimensional setting. Setting $\Omega = [0, L]$, then the eigenvalue is $\lambda_1 = (\pi/L)^2$, and we can rewrite Theorem 2 in the following manner.

Corollary 4 *If $\Omega = [0, L]$, $g \in C^2(\mathbb{R})$, and g is of logistic type (2) and satisfies the subtangential condition (3), then we have two cases:*

1. *If $L \geq \pi\sqrt{\dfrac{d}{g(0)}}$, then (34) has a nontrivial solution;*
2. *If $L < \pi\sqrt{\dfrac{d}{g(0)}}$, then (34) only has the trivial solution.*

In this one-dimensional setting, we have a clear bifurcation in the behavior of solutions based on the domain size L, and denote the bifurcation value for L the *critical domain size*:

$$L_{crit} = \pi\sqrt{\frac{d}{g(0)}}. \tag{35}$$

6.2 The go-or-grow case

Returning to the go-or-grow model (4), similarly to the previous section, we look for nontrivial steady states, which will be nonnegative solutions of the following boundary value problem

$$\begin{cases} -d\Delta u = -\mu u - \alpha(u,v)u + \beta(u,v)v, & \text{in } \Omega, \\ g(u+v)v + \alpha(u,v)u - \beta(u,v)v = 0, & \text{in } \Omega, \\ (u,v) = (0,0), & \text{on } \partial\Omega, \end{cases} \tag{36}$$

where Ω is a bounded domain with a smooth boundary.

The critical domain size problem for the case where α and β are constant (the constant rates go-or-grow model (8)) was studied in Hadeler and Lewis (2002), where the following result was proven.

Theorem 5 *(Theorem 4 in Hadeler and Lewis 2002) Consider (36) with constant rates α and β. If $g \in C^2(\mathbb{R})$, and g is of logistic type (2) and satisfies the subtangential condition (3), then we have three cases:*

1. *Assume $\beta > g(0)$ and*

$$\lambda_1(\Omega) < \frac{1}{d}\left(\frac{\alpha g(0)}{\beta - g(0)} - \mu\right), \tag{37}$$

then there exists a nontrivial steady state solution;

2. *Assume* $\beta > g(0)$ *and*

$$\lambda_1(\Omega) > \frac{1}{d}\left(\frac{\alpha g(0)}{\beta - g(0)} - \mu\right), \tag{38}$$

then the steady state is zero;

3. *If* $\beta < g(0)$*, then the zero solution is always unstable, and nontrivial steady states exist.*

Similar to the FKPP case, we have a bifurcation that is based on the domain size in cases 1 and 2. The threshold in (37)–(38) depends on the growth rate and, somewhat unsurprisingly, on the transition rates α and β and the death rate μ. What is surprising is that a third case appears for a small transition rate β. If the growth rate of the v population at 0 is greater than the transition rate out of the v compartment, i.e., $\beta < g(0)$, then there is no critical domain or bifurcation on the domain size. This means that for any size or shape of domain Ω, there exist nontrivial populations of u and v.

This property is another example of the unexpected properties of the go-or-grow systems. In fact, we can link this case to the autocatalysis condition (27) discussed earlier. If we compute (27) for the constant rates model (8), we find indeed

$$\left.\frac{\partial h}{\partial v}\right|_{(u,v)=(0,0)} = g(0) - \beta > 0.$$

In the autocatalysis case where $\beta - g(0) > 0$, we can directly relate the results from Theorem 2 and Theorem 5 for $\Omega = [0, L]$ and $\mu = 0$. The threshold condition (38) can be written as a condition for the domain length L

$$L > L_{\text{ crit}} = \pi\sqrt{\frac{d(\beta - g(0))}{g(0)\alpha}} = \pi\sqrt{\frac{d}{g(0)}}\underbrace{\sqrt{\frac{\beta - g(0)}{\alpha}}}_{K_{\alpha\beta}}. \tag{39}$$

In this example, the critical domain of FKPP (35) and the critical domain of the constant rates go-or-grow model (39) are related by the factor $K_{\alpha\beta}$. Setting $K_{\alpha\beta} = 1$ gives the equation when the two critical domains are equal, $\alpha + g(0) = \beta$. If we increase the transition rate to the moving population, β, or decrease the transition rate to the growing population, α, from the $K_{\alpha\beta} = 1$ values, the critical domain of the go-or-grow model will be larger than the critical domain of FKPP. Similarly, if we reduce β or increase α, the critical domain of the go-or-grow model will be smaller than the critical domain of FKPP.

7 Traveling wave analysis and invasion speeds

To quantify the spread of populations in terms of the speed of invasion, traveling wave analysis has become a widely adopted approach, with a particular focus on determining the existence of traveling waves and their minimum speed. This is due to the fact that both the FKPP Eq. (1) and go-or-grow models (4) inherently describe situations where waves of population density propagate at a constant speed.

7.1 The FKPP case

The analysis of traveling waves for the FKPP equation (1) is a well-researched and well-described textbook method (Murray 2002; Smoller 1983; Britton 1986; Levin and Okubo 2002; Lewis et al. 2002). Consider (1) on the real line and assume the growth function f is of logistic type (2), we introduce the *traveling wave coordinate* $z = x - ct$ with *wave speed* c, and define a traveling wave solution to be a self-similar solution of the form $m(t, x) = M(z)$. Substituting this ansatz into (1) yields a second-order ODE for M of the form

$$-cM' = dM'' + g(M)M, \tag{40}$$

with boundary conditions $M(-\infty) = 1$ and $M(\infty) = 0$. This ODE can be analyzed with phase plane methods, where a traveling wave of (1) corresponds to a heteroclinic connection between two equilibria in the phase space. This heteroclinic connection depends on the choice of the speed c. As done in Murray (2002); Smoller (1983); Britton (1986); Levin and Okubo (2002); Lewis et al. (2002), it can be shown that, under the subtangential condition (3), the minimum wave speed is

$$\bar{c}_{\mathrm{FKPP}} = 2\sqrt{dg(0)}.$$

7.2 The go-or-grow case

As in the FKPP case, traveling wave solutions for go-or-grow models can be seen as connections between two equilibria of the system. Ahead of the wave, we find the trivial equilibrium $(u, v) = (0, 0)$, while at the back of the wave we typically see a coexistence equilibrium (u^*, v^*). To ensure these states exist, we make the following assumption:

- g is a continuous function that is differentiable at 0 and 1, it has one root at $n = 1$, and

$$g(n)n \leq g(0)n \text{ for } 0 \leq n \leq 1; \tag{41}$$

- there is only one non-zero solution $(u^*, v^*) \in \mathbb{R}^2_+$ of the system

$$\begin{cases} 0 = -\mu u^* - \alpha(u^*, v^*)u^* + \beta(u^*, v^*)v^*, \\ \mu u^* = g(u^* + v^*)v^*. \end{cases} \tag{42}$$

Assumptions (41)–(42) guarantees that $\mathbf{F}(0,0) = \mathbf{F}(u^*, v^*) = (0,0)$ in (10), allowing us to formalize the question of a traveling wave with the following definitions.

Definition 2 Consider the general go-or-grow model (4) and introduce the *traveling wave coordinate* $z = x - ct$ for a fixed speed c. A solution of the form $u(t,x) = U(x-ct)$ and $v(t,x) = V(x-ct)$ is called a *traveling wave solution with speed c*. The traveling wave is called a *wave front* if $\big(U(z), V(z)\big)$ has limits

$$\lim_{z\to+\infty} \big(U(z), V(z)\big) = (0,0), \quad \lim_{z\to-\infty} \big(U(z), V(z)\big) = (u^*, v^*).$$

If $c > 0$, the invading traveling wave moves to the right, while if $c < 0$, the invading traveling wave moves to the left.

There are two distinct notions for the wave speed, c, which are relevant in our analysis.

Definition 3

- The *nonlinear spread rate*, c^*, denotes the observed minimal spreading speed of solutions of the full nonlinear system (4).
- The *linear spread rate*, $\bar{c}$, denotes the spreading wave speed of the solutions of its linearization at the leading edge (see Hadeler and Lewis 2002).

Specifically, we say that the system is *linearly determined* if $c^* = \bar{c}$.

The first results for the existence of wave fronts and the expression for the corresponding spreading speed were obtained for the constant rates go-or-grow model (8) by Hadeler, Lewis, and collaborators (Lewis and Schmitz 1996; Hadeler and Lewis 2002). The connection between nonlinear spread speed, c^*, and linear spread speed, $\bar{c}$, was established in the case that the function $g(u+v)$ only depends on the stationary population $g(v)$.

For the balanced go-or-grow model (7) with $g(n) = 1 - n$, Pham (2012) showed numerically that invasion waves exist with different qualitative behavior. In particular, the wake of the wave might be a homogeneous steady state, a periodic wave train, or even an irregular pattern, as we have shown in Sect. 5.

More recently, Falcó et al. (2024) examined the minimum invasion speed in the case of the total population go-or-grow model (6) with no death rate ($\mu = 0$), logistic growth for the proliferating population ($g(n) = 1 - n$), and $\alpha(n)$ and $\beta(n)$ as nonincreasing and nondecreasing functions, respectively. By assuming $\alpha(n) > 0$ for all $n > 0$, they ensure the existence of only two equilibria in the system,

$$E_0 = (0,0), \qquad E_1 = \left(\frac{\beta(1)}{\alpha(1)+\beta(1)}, \frac{\alpha(1)}{\alpha(1)+\beta(1)}\right),$$

and find the traveling wave solutions as heteroclinic connections between these two equilibria in phase space. Moreover, considering the linearized version of (6) about the equilibrium E_0 and transforming to wave coordinates, they obtain the expression for the linear spread rate

$$\bar{c} = \inf_{\rho>0} \frac{\rho^2 + 1 - \alpha(0) - \beta(0) + \sqrt{\left(\rho^2 + 1 - \alpha(0) - \beta(0)\right)^2 - 4\left(1-\beta(0)\right)\rho^2 + 4\alpha(0)}}{2\rho}. \quad (43)$$

Although this formula still includes the infimum operation, it is observed that

$$\frac{dc}{d\rho}(\rho)\Big|_{\rho=1} = \frac{\beta(0)-\alpha(0)}{\alpha(0)+\beta(0)},$$

and thus, some special cases emerge.

- For $\alpha(0) = \beta(0)$, (43) obtains its minimum at $\rho = 1$, which implies that $\bar{c} = 1$.
- For $\beta(0) = 0$, it is possible to explicitly solve (43), obtaining

$$\bar{c} = \frac{1}{\sqrt{1+\alpha(0)}}.$$

  In this case, if $\beta(n) \neq 0$ for $n > 0$, it has been demonstrated that ensuring the positivity of traveling wave solutions requires a wave speed $c > \bar{c}$. Therefore, for the case where $\beta(0) = 0$, the traveling wave solutions exhibit a wave speed greater than $\bar{c}$ meaning that the wave speed is nonlinearly determined.

- Similarly, if $\alpha(0) = 0$,

$$\bar{c} = \begin{cases} \sqrt{1-\beta(0)}, & \text{if } \beta(0) < 1, \\ 0, & \text{otherwise.} \end{cases}$$

- When $\alpha(0) \neq \beta(0)$, $\bar{c} \leq c(1) = 1$.

Similar results for the total population go-or-grow model (6) were obtained in Stepien et al. (2018) in the case $\mu \neq 0$, assuming logistic growth with constant rate, r, and the following specific forms for the transition functions,

$$\alpha(n) = \kappa \frac{K_v^k}{n^k + K_v^k}, \qquad \beta(n) = \epsilon\kappa \frac{n^k}{n^k + K_u^k}, \quad (44)$$

with ϵ, κ, k, K_u, and K_v positive constants. A closed form for the dispersion relation was obtained, which provides the minimum wave speed

$$\bar{c} = r\sqrt{\frac{d}{r+\kappa+\mu}}. \tag{45}$$

Moreover, the existence of a heteroclinic orbit in phase space that corresponds to the approximate traveling wave (under certain conditions) was proven.

7.3 A unifying framework and a general result

The previous results can be cast into the framework of cooperative reaction–diffusion systems. The lemmas and theorems presented here are new, and they are based on a general theory of cooperative reaction–diffusion systems developed in Liang and Zhao (2007); Fang and Zhao (2009); Weinberger et al. (2002). The proofs require a check of the general assumptions, which is presented in Appendix A.

Before we show the existence of traveling waves, we first characterize the wave speed $\bar{c}$ through the linearization at the leading edge. For this, we make the following assumptions:

- $\alpha(u,v)$ and $\beta(u,v)$ are piecewise continuously differentiable in (u,v) for $0 \le u \le u^*$and $0 \le v \le v^*$, differentiable at $(0,0)$, and

$$(g(0)-\beta(0,0))(\mu+\alpha(0,0))+\alpha(0,0)\beta(0,0) > 0; \tag{46}$$

- For any $(u,v) \in [0,u^*] \times [0,v^*]$,

$$\begin{aligned} &\alpha(u,v)+\frac{\partial}{\partial u}(\alpha(u,v))u+\frac{\partial}{\partial u}(g(u+v)-\beta(u,v))v \ge 0, \text{ and} \\ &\beta(u,v)+\frac{\partial}{\partial v}(\beta(u,v))v-\frac{\partial}{\partial v}(\alpha(u,v))u \ge 0. \end{aligned} \tag{47}$$

Assumption (46) gives regularity such that we can take the Jacobian at $(0,0)$ and ensures that the Jacobian at $(0,0)$ has a positive eigenvalue. Note that, if $\mu = 0$, the condition $(g(0)-\beta(0,0))(\mu+\alpha(0,0))+\alpha(0,0)\beta(0,0) > 0$ is satisfied. The assumption (47) is sufficient to ensure that (4) is cooperative.

We transform system (10) into wave coordinates $z = x - ct$ and linearize about $(0,0)$ to obtain

$$-c\mathbf{w}' = D\mathbf{w}'' + \mathbf{F}'(0,0)\mathbf{w}, \tag{48}$$

where $\mathbf{w} = (u,v)^T$, $D = \text{ diag }(d,0)$, $\mathbf{F}$ is as defined in (11), and $\mathbf{F}'(0,0)$ is the Jacobian of $\mathbf{F}$ at $(0,0)$. We write the solution of (48) as $\mathbf{w} = \boldsymbol{\nu} e^{-\rho z}$, where ρ denotes the exponential decay rate at the leading edge and $\boldsymbol{\nu}$ is an arbitrary vector. Substituting this ansatz into (48) yields the algebraic system

$$-c\rho\boldsymbol{\nu} = D\rho^2\boldsymbol{\nu} + \mathbf{F}'(0,0)\boldsymbol{\nu}.$$

Defining the matrix $A(\rho) = D\rho^2 + \mathbf{F}'(0,0)$, we arrive at the eigenvalue problem given by

$$(A(\rho) - c\rho\mathbb{I})\boldsymbol{\nu} = 0,$$

for the eigenvalue $\lambda_A = c\rho$. We find that the principal and positive eigenvalue of A is

$$\lambda_A(\rho) = \frac{d\rho^2 + g(0) - \mu - \alpha(0,0) - \beta(0,0)}{2} + \frac{\sqrt{\left[d\rho^2 + g(0) - \mu - \alpha(0,0) - \beta(0,0)\right]^2 + 4\left[(g(0) - \beta(0,0))(\mu + \alpha(0,0) - d\rho^2) + \alpha(0,0)\beta(0,0)\right]}}{2}, \tag{49}$$

with associated eigenvector

$$\boldsymbol{\nu}(\rho) = \left(\frac{\lambda_A(\rho) - g(0) + \beta(0,0)}{\alpha(0,0)},\ 1\right)^T, \tag{50}$$

which is a positive vector for all $\rho \geq 0$. To find the minimum wave speed of the linearized system, $\bar{c}$, we take the minimum ratio of the eigenvalue and decay rate as

$$\bar{c} := \inf_{\rho > 0} \frac{\lambda_A(\rho)}{\rho}. \tag{51}$$

We verified that, under the assumptions $\mu = 0$, $\alpha = \alpha(n)$, and $\beta = \beta(n)$, condition (51) coincides with (43) derived in Falcó et al. (2024) for the total population model (6). Furthermore, when $\mu \neq 0$ and the transition functions are given by (44), condition (51) matches (45), which was previously derived in Stepien et al. (2018).

Lemma 6 *Let α, β, and g satisfy (41), (42), (46), and (47) and consider the initial condition $\phi = (\phi_1, \phi_2) \in \mathcal{C}_{u^*,v^*} = \{(\phi_1, \phi_2) \in C(\mathbb{R}; \mathbb{R}^2) : 0 \leq \phi_1(z) \leq u^*,\ 0 \leq \phi_2(z) \leq v^*\ \forall z \in \mathbb{R}\}$. Let $\mathbf{w}(t, x; \phi) := \big(u(t, x; \phi_1), v(t, x; \phi_2)\big)$ be the unique solution of (4) through ϕ. Then, there exists a real number c^* with $0 < c^* \leq \bar{c}$, such that the following statements are valid:*

1. *If ϕ has compact support, then* $\lim_{\substack{t \to \infty \\ |x| \geq ct}} \mathbf{w}(t, x; \phi) = 0$, *for all $c > c^*$;*
2. *For any $c \in (0, c^*)$ and $\mathbf{r} > \mathbf{0}$, there is a positive number $R_{\mathbf{r}}$ such that for any $\phi \in \mathcal{C}_{u^*,v^*}$ with $\phi \leq \mathbf{r}$ on an interval of length $2R_{\mathbf{r}}$, there holds*

$$\lim_{\substack{t \to \infty \\ |x| \leq ct}} \mathbf{w}(t, x; \phi) = (u^*, v^*);$$

3. *If, in addition, we have a linear bound for any $\eta > 0$, i.e.,*

$$g\big(\eta(1+\nu_1(\rho))\big) \le -\alpha\big(\eta\nu_1(\rho),\eta\big)\nu_1(\rho) + \beta\big(\eta\nu_1(\rho),\eta\big) + \lambda_A(\rho) \le g(0), \quad (52)$$

for all $\rho \in (0,\rho^*]$, then $c^* = \bar{c}$, where ρ^* is the value of ρ at which $\lambda_A(\rho)/\rho$ attains its infimum, and $\nu_1(\rho)$ is the first component of the eigenvector (50).

Proof The proof is based on the general theory of Liang and Zhao (2007); Fang and Zhao (2009); Weinberger et al. (2002) and is presented in Appendix A. □

Lemma 6 provides sufficient conditions for the existence of a constant spreading speed of a compact initial condition in items 1 and 2. Item 3 gives conditions such that the model is linearly determined and that the nonlinear spread rate, c^*, coincides with the linearized spread rate, $\bar{c}$. However, to prove the existence of traveling waves, we also require condition (52) as well as the following assumption:

- There exist $a > 0$, $\sigma > 1$, and $\boldsymbol{r} > \mathbf{0}$ such that

$$\begin{aligned}&(\alpha(0,0)-\alpha(u,v))u + (\beta(u,v)-\beta(0,0))v \ge -a|u+v|^\sigma,\\ &(g(u+v)-g(0))v - (\alpha(0,0)-\alpha(u,v))u - (\beta(u,v)-\beta(0,0))v \ge -a|u+v|^\sigma,\\ &\text{for all } \mathbf{0} \le (u,v) \le \mathbf{r}.\end{aligned} \quad (53)$$

Although condition (53) looks quite complex, it is already satisfied when $\mathbf{F}(u,v)$ is twice differentiable in both components (Fang and Zhao 2009). The assumption (52) comes from a variant of the subtangential condition (3), see (70) in the appendix. With assumptions, (41)–(42), (46)–(47), and (52)–(53), we can show that (4) has traveling wave solutions.

Theorem 7 *If the general grow-or-grow model (4) satisfies the conditions, (41)–(42), (46)–(47), and (52)–(53), then for each $c < \bar{c}$, it has a nonincreasing wavefront $\big(U(x-ct), V(x-ct)\big)$ connecting (u^*, v^*) to $(0,0)$. However, for any $c \in (0,\bar{c})$, there is no wavefront $\big(U(x-ct), V(x-ct)\big)$ connecting (u^*, v^*) to $(0,0)$.*

Proof The proof requires a check that the conditions for the general theory of cooperative systems are satisfied, and it is presented in Appendix A. □

Theorem 7 allows us to establish the existence of traveling wave solutions with a formula for the wave speed (51) for a large class of go-or-grow models. Although many go-or-grow models fall into the above framework, there exists plenty of examples that fail one of the assumptions, such as those studied in Stepien et al. (2018); Tursynkozha et al. (2023); Falcó et al. (2024) that numerically display traveling wave solutions, but they fail the cooperativity condition (46). To prove traveling wave solutions in those cases, one can attempt to construct upper and lower solutions and use a fixed point proof, as done in Zhang (2017); Zhang et al. (2016); Zhang and Wang (2014), or use a geometric shooting method, as in Li and Wu (2008); Hsu et al. (2012); Huang et al. (2003); Lin et al. (2011); Huang (2012, 2016). Another common method is to use approximations, such as the fast transition rate scaling introduced in

Sect. 3.3, where the general go-or-grow model (4) can be transformed into a FKPP equation (1) for the total population depending on the form of the transition functions α and β. Since the FKPP equation (1) has traveling wave solutions and a simple formula for the spreading speed, the fast-transition scaling can provide an approximation on the spreading speed of (4).

7.4 Connection between the spread rate of the FKPP equation and go-or-grow models

To link the foundational analysis of the FKPP equation (1) as summarized in Sect. 7.1 with analysis of go-or-grow types of models (10) (Sects. 7.2–7.3), we compare the spread rate between the cases.

Theorem 8 *Assume $\mu = 0$, $\mathbf{F}(\mathbf{w})$ is given by (11), and α, β, and g satisfy assumptions (41)–(42), (46)–(47), and (52)–(53). Then the minimum wave speed, $\bar{c}$ of the go-or-grow model (4) given by (51) satisfies the inequality*

$$\bar{c} \leq \frac{1}{2}\bar{c}_{FKPP} = \sqrt{dg(0)}. \tag{54}$$

Proof Since $\mathbf{F}(u, v)$ satisfies assumptions, (41)–(42), (46)–(47), and (52)–(53), Theorem 7 can be applied, and we have that the minimum wave speed of the corresponding go-or-grow model is given by

$$\bar{c} = \inf_{\rho \geq 0} \frac{\lambda_+(\rho)}{\rho}, \tag{55}$$

where $\lambda_+(\rho)$ is the principal eigenvalue of the matrix

$$A = \begin{pmatrix} d\rho^2 & 0 \\ 0 & 0 \end{pmatrix} + \begin{pmatrix} -\alpha(0,0) & +\beta(0,0) \\ \alpha(0,0) & -\beta(0,0) + g(0) \end{pmatrix}. \tag{56}$$

This can be written explicitly as

$$\begin{aligned} \lambda_+(\rho) = {} & \frac{d\rho^2 + g(0) - \alpha(0,0) - \beta(0,0)}{2} \\ & + \frac{\sqrt{\left(d\rho^2 + g(0) - \alpha(0,0) - \beta(0,0)\right)^2 - 4\left(d\rho^2(g(0) - \beta(0,0)) - \alpha(0,0)g(0)\right)}}{2}. \end{aligned} \tag{57}$$

We notice that substituting the choice of $\rho = \sqrt{g(0)/d}$ into (57), we get

$$\frac{\lambda_+\left(\sqrt{\frac{g(0)}{d}}\right)}{\sqrt{\frac{g(0)}{d}}} = \sqrt{dg(0)}.$$

Thus, we have the set of inequalities

$$\bar{c} = \inf_{\rho \geq 0} \frac{\lambda_+(\rho)}{\rho} \leq \sqrt{dg(0)} \leq 2\sqrt{dg(0)} = \bar{c}_{\text{FKPP}}. \tag{58}$$

□

Some special cases of this result were already proven in the literature for the constant rates model (8) in Fedotov and Iomin (2008); Lewis and Schmitz (1996) and for the total population model (6) in Falcó et al. (2024). However, the results provided here are a generalization for the case of the general go-or-grow model (4). As an example, in Fig. 6 we illustrate the traveling wave profile for the constant rates model (8) (black and red curves) and the FKPP model (1) (blue curves). These numerical simulations show how the FKPP model is at least two times faster than the constant rates go-or-grow model.

7.5 Large wave speed scaling

In addition to studying the wave speed of traveling wave solutions of the general go-or-grow model (4), here we introduce the large wave speed scaling approach, which provides insights into the shape of the traveling waves. Originally developed by Canosa (1973), this method allows for an approximation of the traveling wave solution by considering an asymptotic expansion of the traveling wave system in the limit of large wave speeds. For systems for which no general traveling wave solution theory exists, i.e., those systems which are noncooperative and not bounded above and below by cooperative systems, this technique is a useful way to obtain the form of the traveling wave by solving a much simpler approximate system. Furthermore, this approach facilities the investigation of the conditions under which the approxi-

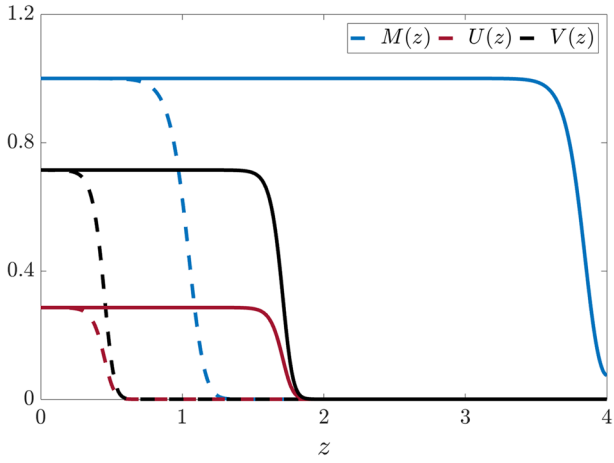


Fig. 6 Traveling wave profiles for models (1) and (8). Traveling wave profiles for the FKPP model (1) ($M(z)$in blue) and the constant rate go-or-grow (8) (moving cells $U(z)$ in red, proliferating cells $V(z)$ in black). Simulations are shown at two different time steps: an earlier time T_1 (dashed curves) and a later time T_2 (solid curves). Parameters are set to $\alpha = 1$, $\beta = 2$, $g(0) = 1$, $\mu = 0$, and $d = 0.0001$.

mation aligns closely with the traveling wave system, providing a clearer understanding of the wave dynamics.

Introducing the traveling wave coordinate, $z = x - ct$, such that $U(z) = u(t, x)$ and $V(z) = v(t, x)$, the general go-or-grow model (4) is written as

$$\begin{cases} -cU' = DU'' - \mu U - \alpha(U, V)U + \beta(U, V)V, \\ -cV' = g(U + V)V + \alpha(U, V)U - \beta(U, V)V. \end{cases} \tag{59}$$

By using the scaling $\xi = -\frac{1}{c}z$, we obtain the approximation

$$\begin{cases} U' = \dfrac{D}{c^2}U'' - \mu U - \alpha(U, V)U + \beta(U, V)V, \\ V' = g(U + V)V + \alpha(U, V)U - \beta(U, V)V. \end{cases}$$

Defining the perturbation parameter $\delta := 1/c^2$ and assuming it is small, we expand U and V as regular perturbation expansions

$$U = \sum_{n=0}^{\infty} U_n \delta^n, \qquad V = \sum_{n=0}^{\infty} V_n \delta^n.$$

As in the fast transition rate scaling (Sect. 3.3), we require that α, β, and g are sufficiently smooth to allow for a Taylor expansion at (U_0, V_0). In addition, we require each order of δ to vanish independently. With both of these assumptions, the zeroth order of δ reads

$$\begin{cases} U_0' = -\mu U_0 - \alpha(U_0, V_0)U_0 + \beta(U_0, V_0)V_0, \\ V_0' = g(U_0 + V_0)V_0 + \alpha(U_0, V_0)U_0 - \beta(U_0, V_0)V_0. \end{cases} \tag{60}$$

The effective result of scaling is removing the diffusion term from the analysis, reducing the dimension of the phase space of the problem by one. In this case, we reduce the phase space to two dimensions, allowing for the examination of the shape of the traveling wave solutions.

Example We illustrate the large wave speed approximation in the case of the constant rates go-or-grow model (8) with $\mu = 0$ and logistic growth function, $g(u + v)v = (1 - (u + v))v$. In this example, system (60) becomes

$$\begin{cases} U_0' = -\alpha U_0 + \beta V_0, \\ V_0' = (1 - U_0 - V_0)V_0 + \alpha U_0 - \beta V_0. \end{cases} \tag{61}$$

The classical phase plane analysis shows that the origin $(0, 0)$ is a saddle node and the equilibrium $(U_0^*, V_0^*) = \left(\frac{1}{\alpha/\beta+1}, \frac{\alpha/\beta}{\alpha/\beta+1}\right)$ is a stable node. We calculate the nullclines of the above system in terms of U_0, obtaining

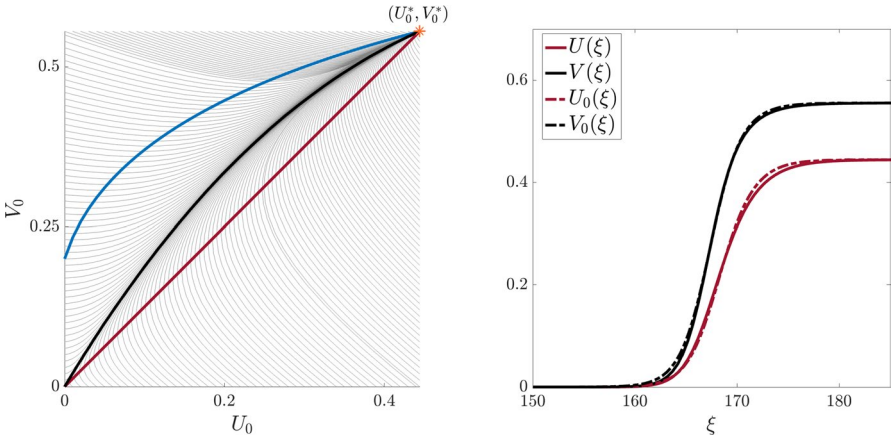


Fig. 7 Large wave speed scaling applied to model (8). (Left) Phase portrait of system (61). Trajectories are depicted in light grey, while the blue curve represents the V_0 nullcline (63), the red curve represents the U_0 nullcline (62), and the black curve represents the heteroclinic connection from the $(0, 0)$ equilibrium to (U_0^*, V_0^*) (orange marker). (Right) Comparison between the traveling wave profile (solid curves) from the model (8) with the corresponding large wave speed approximation (61) (dot-dashed curves) in the coordinate ξ. Logistic growth is assumed in (8), and the parameters (for both plots) are set to $\alpha = 1$, $\beta = 0.8$, $\mu = 0$, and $d = 0.0001$.

$$U_0\text{-nullcline:} \qquad V_{\mathcal{N}_1}(U_0) = \frac{\alpha}{\beta} U_0, \tag{62}$$

$$V_0\text{-nullcline:} \qquad V_{\mathcal{N}_2}(U_0) = \frac{(1-U_0)-\beta}{2} + \frac{\sqrt{((1-U_0)-\beta)^2 + 4\alpha U_0}}{2}. \tag{63}$$

From these nullclines, it is possible to define the trapping region

$$\mathcal{W} = \{(U_0, V_0) \in \mathbb{R}_+^2 : 0 \leq U_0 \leq U_0^*,\ V_{\mathcal{N}_1}(U_0) \leq V_0 \leq V_{\mathcal{N}_2}(U_0)\}. \tag{64}$$

Indeed, for trajectories on the line $\{U_0 = 0,\ V_0 > 0\}$, we have $U_0' > 0$, thus they point inward into $\mathcal{W}$. Then, we consider the curve $\{V_0 = V_{\mathcal{N}_1}(U_0),\ 0 < U_0 < U_0^*\}$, whose trajectories have $U_0' = 0$ and

$$V_0' = \frac{\alpha}{\beta}\left[1 - \left(1 + \frac{\alpha}{\beta}\right) U_0\right] U_0 > 0,$$

thus, the flux points upwards into $\mathcal{W}$. Finally, on the curve $\{V_0 = V_{\mathcal{N}_2}(U_0),\ 0 < U_0 < U_0^*\}$, the trajectories have $V_0' = 0$ and

$$U_0' = -\alpha U_0 + \beta V_{\mathcal{N}_2}(U_0) > -\alpha U_0 + \beta V_{\mathcal{N}_1}(U_0) = 0,$$

meaning that the flux points into $\mathcal{W}$. Therefore, by Poincaré–Bendixson theorem (Theorem 3.7.1 in Perko 2013), we have that every ω-limit set of a trajectory inside $\mathcal{W}$ is either a fixed point, a periodic orbit, or a heteroclinic orbit between the two

fixed points $(0,0)$ and (U_0^*, V_0^*). Considering the Dulac function $\phi = -1/V$, we can rule out periodic orbits by applying Dulac's criterion (Theorem 3.9.2 in Perko 2013). Thus, we obtain the existence of a heteroclinic orbit between $(0,0)$ and (U_0^*, V_0^*). Figure 7 illustrates the phase portrait of the system (61) and the heteroclinic orbit between the two equilibria on the left, as well as the heteroclinic orbit and the traveling wave solution of (61) in the wave coordinate ξ on the right.

The large wave speed scaling has been used extensively in mathematical biology, especially in cancer growth models Sherratt by (2000); Sherratt and Chaplain (2001); Zhu et al. (2008); Quinn and Sinkala (2009); Zhu and Ou (2011). It was explicitly used for the total population go-or-grow models in Stepien et al. (2018); Tursynkozha et al. (2023) for obtaining an approximation of the traveling wave solution. In particular, in Stepien et al. (2018), the authors numerically show that for small values of the wave speed, the simulations do not agree, while for larger values of wave speed they observe that the approximation is valid.

8 Discussion

In this article, we have examined the significance of a class of go-or-grow models that are widely employed to describe various biological phenomena, particularly those related to cell dynamics and cancer progression. What started as a simple review of go-or-grow models quickly became a mathematically involved exposition. Our primary objective has been to provide a comprehensive review of the intriguing mathematical features that characterize this approach, while also highlighting the challenges and open problems that may inspire future mathematical investigations. Despite the biological relevance of these models and their extensive application across various mathematical contexts, a systematic exploration of their mathematical properties and the associated analytical and numerical challenges has been lacking. While we do not claim our analysis is exhaustive, we have endeavored to delve into the diverse array of analytical results available in the literature, examining different mathematical assumptions related to the switching terms of the models and establishing clear connections between the classical FKPP equation and its go-or-grow counterparts.

Beginning with a brief overview of the biological evidence for the emergence of dichotomic dynamics in biological systems, we focused specifically on glioma cell evolution. Research has demonstrated that the progression of this tumor is driven by a proliferation/migration dichotomy, where proliferating cells remain stationary or move slowly, while migrating cells do not proliferate Giese (1996); Giese et al. (2003). This serves as the primary biological motivation for our exploration of this class of models. We provided a comprehensive summary of the extensive mathematical literature addressing the go-or-grow dichotomy in glioma progression, spanning from stochastic and discrete approaches to continuous frameworks, with migratory dynamics and population switches influenced by various external and intrinsic factors.

We focused on a specific continuous modeling framework, which we named as the *general go-or-grow model* (4). This model features linear diffusion for the mov-

ing population and a characteristic switch between the two populations: migrating cells (u) and proliferating (v) cells. The transition functions $\alpha(\cdot)$ and $\beta(\cdot)$ govern this switching and depend solely on the densities of the populations. Depending on the nature of this dependency, we proposed various specialized versions of the model and reviewed the key papers that have contributed to their analysis. Moreover, we revisited a general existence result for the general model and discussed common scaling techniques that facilitate its analysis, particularly in relation to the classical FKPP equation.

Although these go-or-grow models have been widely employed, they present a range of analytical and numerical challenges associated with the emergence of highly unstable patterns and irregular traveling waves under specific assumptions on the transition functions. While these issues have been observed in different contexts (Pham 2012; Härting and Marciniak-Czochra 2014), we highlighted and integrated them into a common framework. Singularities arise, driven by an extreme version of the Turing instability, where the diffusion coefficient of the activator is zero. All high frequencies are unstable, leading to oscillations and patterns on fine scales. Of course, this instability has conditions, and if these conditions are not satisfied, then the model is well-behaved.

Focusing on specific analytical properties of go-or-grow models that can be effectively addressed, we extensively reviewed results related to the critical domain problem and the analysis of the existence and minimal speed of traveling wave solutions for the general go-or-grow model and its specialized variants. For the critical domain problem, we revisited classical results concerning the FKPP equation (Britton 1986; Wang and Pang 2024) and connected them to findings related to the general go-or-grow model, which show the bifurcation between domain size and the existence of non-trivial steady-state solutions, under specific assumptions about the transition and growth functions. In our examination of traveling wave solutions, we outlined the necessary assumptions that the general go-or-grow model (4) must meet to be classified as a cooperative system. This classification allows us to apply a robust theoretical framework concerning the existence of traveling waves and invasion speed, as established in the literature (Fang and Zhao 2009; Weinberger et al. 2002). Similar to our analysis of the critical domain size, we establish a connection to the FKPP equation, thereby generalizing previous results to the context of the general go-or-grow model (4) introduced here.

Open Problems While we have reviewed a wide array of analytical and numerical results concerning this special class of mathematical models, several important mathematical questions remain unresolved. One intriguing question that arises from our analysis pertains to the convergence of the fast-transition rate system (12) to system (16) as $\varepsilon \to 0$, specifically in the context of traveling wave solutions: what assumptions must be satisfied for the limit $\varepsilon \to 0$ to ensure convergence (in some sense) of (12) to (16)? Furthermore, if (12) meets these necessary conditions, what does the wave speed of (12) converge to in this limit? How does this relate to the minimum wave speed of the corresponding FKPP equation given by (17)?

Similar questions arise when considering large wave speed scaling. Many biological systems can be described by models of the form (4), with specific expressions for the transition functions $\alpha(u, v)$ and $\beta(u, v)$ that may result in noncooperative dynam-

ics. Under what conditions is the existence of traveling waves guaranteed in these noncooperative models, and what is the minimum wave speed associated with them? For cooperative systems, when can we derive an explicit expression for the minimum wave speed, as indicated in (51)?

Additional challenges emerge from the instabilities and patterns discussed in Sect. 5. How can the autocatalysis condition (27) be formulated for a general model within the go-or-grow family? Is it feasible to develop more sophisticated numerical solvers capable of correctly identifying the sources of the observed instabilities?

These open questions present intriguing opportunities for future research. As we intended to showcase the usefulness of go-or-grow modeling in biology while highlighting interesting mathematical properties, this article is also a warning not to underestimate the monster on a leash.

A. Appendix: Proofs of Lemma 6 and Theorem 7

The proofs of Lemma 6 and Theorem 7 primarily require showing that the general go-or-grow model (4) with the assumptions, (41)–(42), (46)–(47), and (52)–(53) lives inside the general cooperative theory proposed by Liang and Zhao (2007); Fang and Zhao (2009); Weinberger et al. (2002). In these works, the authors are concerned the n-equation reaction–diffusion system

$$\mathbf{w}_t = D\Delta\mathbf{w} + \mathbf{F}(\mathbf{w}), \tag{65}$$

where $\mathbf{w} = (w_1, \ldots, w_n)$ and $D = \mathrm{diag}(d_1, \ldots, d_n)$, with $d_i \geq 0$ and at least one $d_i \neq 0$. Moreover, we require the following assumptions on the reaction term $\mathbf{F} : \mathbb{R}^n \longrightarrow \mathbb{R}^n$:

- $\mathbf{F}$ is continuous with

$$\mathbf{F}(\mathbf{0}) = \mathbf{F}(\overline{\mathbf{w}}) = \mathbf{0}, \tag{66}$$

  and there is no $\mathbf{u}$ such that $\mathbf{F}(\mathbf{u}) = 0$ and $\mathbf{0} < \mathbf{u} < \bar{\mathbf{w}}$;

- The system is cooperative

$$i.e., \text{each component } f_i \text{ of } \mathbf{F} \text{ is nondecreasing in all the components of } \mathbf{w}, \tag{67}$$

  with the possible exception of the i th one;

- $\mathbf{F}(\mathbf{w})$ is piecewise continuously differentiable in $\mathbf{w}$ for $\mathbf{0} \leq \mathbf{w} \leq \overline{\mathbf{w}}$ and differentiable

$$\text{at } \mathbf{0} \text{ and the matrix } \mathbf{F}'(\mathbf{0}) \text{is irreducible with a positive eigenvalue;} \tag{68}$$

- There exists $a > 0$, $\sigma > 1$, and $\boldsymbol{r} > \mathbf{0}$ such that

$$\mathbf{F}(\mathbf{w}) \geq \mathbf{F}'(\mathbf{0})\mathbf{w} - a\,\|\mathbf{w}\|^{\sigma}\,\mathbf{1}, \tag{69}$$

  for all $\mathbf{0} \leq \mathbf{w} \leq \mathbf{r}$, where $\mathbf{1}$ denotes the vector with all entries equal to 1;

- For any $\eta \geq 0$

$$\mathbf{F}(\min\{\eta\mathbf{w}(\rho), \mathbf{1}\}) \leq \eta D\mathbf{F}(\mathbf{0})\mathbf{w}(\rho), \tag{70}$$

for all $\rho \in (0, \rho^*]$, , where $\rho^*$is the value of ρ at which $\lambda_+(\rho)/\rho$ attains its infimum.

In all the assumptions, the operations are defined component-wise. We show in the following lemma that the general go-or-grow model (4), with the appropriate assumptions, is a special case of the reaction–diffusion equation (65).

Lemma 9 *If the general go-or-grow model* (4) *satisfies* (41)–(42), (46)–(47), *and* (52)–(53), *then* (4) *also satisfies the set of assumptions* (66)–(70).

Proof Condition (66), and the first part of condition (68) are directly satisfied by the assumptions (41)–(42) and (46). In addition, during the wavefront calculation (Sect. 7.3), we computed the eigenvalue of the matrix $A = \rho^2 D + \mathbf{F}'(0,0)$ (48), which for $\rho = 0$ reads

$$\begin{aligned}\lambda_A(0) =& \frac{g(0) - \mu - \alpha(0,0) - \beta(0,0)}{2} \\ &+ \frac{\sqrt{\left[g(0) - \mu - \alpha(0,0) - \beta(0,0)\right]^2 + 4\left[(g(0) - \beta(0,0))(\mu + \alpha(0,0)) + \alpha(0,0)\beta(0,0)\right]}}{2} \\ &> \frac{g(0) - \mu - \alpha(0,0) - \beta(0,0)}{2} + \frac{\sqrt{\left[g(0) - \mu - \alpha(0,0) - \beta(0,0)\right]^2}}{2} \geq 0\end{aligned}$$

completing the requirements for (68).

For assumption (67), consider the Jacobian of $\mathbf{F}$ with components

$$\begin{aligned}\mathbf{F}'_{11}(u,v) &= -(\mu - \alpha(u,v)) - \frac{\partial}{\partial u}(\alpha(u,v))u + \frac{\partial}{\partial u}\beta(u,v)v, \\ \mathbf{F}'_{12}(u,v) &= \beta(u,v) - \frac{\partial}{\partial v}\alpha(u,v)u + \frac{\partial}{\partial v}(\beta(u,v))v, \\ \mathbf{F}'_{21}(u,v) &= \alpha(u,v) + \frac{\partial}{\partial u}(\alpha(u,v))u + \frac{\partial}{\partial u}(g(u+v) - \beta(u,v))v, \\ \mathbf{F}'_{22}(u,v) &= (g(u+v) - \beta(u,v)) + \frac{\partial}{\partial v}(g(u+v) - \beta(u,v))v + \frac{\partial}{\partial v}\alpha(u,v)u.\end{aligned}$$

The cooperativity assumption is satisfied by having the off-diagonal terms greater than or equal to zero, which is exactly assumption (47).

Now, the more technical assumptions (69) and (70) need to be satisfied. Considering the first inequality of assumption (53), rearranging terms, and adding $-\mu\, u$ to both sides yields

$$-(\mu+\alpha(u,v))u+\beta(u,v)\geq -(\mu+\alpha(0,0))u+\beta(0,0)v-a|u+v|^{\sigma},$$

which is exactly $\mathbf{F}_1(u,v)\geq \big(\mathbf{F}'_{11}(0,0),\mathbf{F}'_{12}(0,0)\big)\cdot\begin{pmatrix}u\\ v\end{pmatrix}-a|u+v|^{\sigma}$. For the second component, considering the second inequality of assumption (53) and rearranging terms yields

$$g(u+v)v+\alpha(u,v)u-\beta(u,v)v\geq g(0)-\alpha(0,0)u+\beta(0,0)v-a|u+v|^{\sigma},$$

which is exactly $\mathbf{F}_2(u,v)\geq \big(\mathbf{F}'_{21}(0,0),\mathbf{F}'_{22}(0,0)\big)\cdot\begin{pmatrix}u\\ v\end{pmatrix}-a|u+v|^{\sigma}$. Finally for assumption (70), we compute

$$\begin{aligned}\mathbf{F}'(0,0)\boldsymbol{\nu}(\rho)&=\begin{pmatrix}-(\mu-\alpha(0,0)) & \beta(0,0)\\ \alpha(0,0) & g(0)-\beta(0,0)\end{pmatrix}\begin{pmatrix}\dfrac{\lambda_A(\rho)-g(0)+\beta(0,0)}{\alpha(0,0)}\\ 1\end{pmatrix}\\ &=\begin{pmatrix}g(0)-\mu\nu_1(\rho)-\lambda_A(\rho)\\ \lambda_A(\rho)\end{pmatrix}.\end{aligned}$$

For the first component, taking the middle inequality of assumption (52), i.e.,

$$-\alpha\big(\eta\nu_1(\rho),\eta\big)\nu_1(\rho)+\beta\big(\eta\nu_1(\rho),\eta\big)\leq g(0)-\lambda_A(\rho),\tag{71}$$

adding $-\mu\nu_1(\rho)$ to both sides, and multiplying by $\eta>0$, we get

$$-\alpha\big(\eta\nu_1(\rho),\eta\big)\eta-\mu\nu_1(\rho)\eta+\beta\big(\eta\nu_1(\rho),\eta\big)\eta\leq\big(g(0)-\mu\nu_1(\rho)-\lambda_A(\rho)\big)\eta.$$

Notice that this inequality is exactly

$$\mathbf{F}_1(\eta\nu_1(\rho),\eta)\leq\eta\big(\mathbf{F}'_{11}(0,0),\mathbf{F}'_{12}(0,0)\big)\cdot(\eta\nu_1(\rho),\eta)^T.$$

For the second component, we consider the first inequality of assumption (52), i.e.,

$$g\big(\eta+\eta\nu_1(\rho)\big)\leq-\alpha\big(\eta\nu_1(\rho),\eta\big)+\beta\big(\eta\nu_1(\rho),\eta\big)+\lambda_A(\rho).$$

Rearranging terms and multiplying by η, we get

$$\alpha\big(\eta\nu_1(\rho),\eta\big)\eta-\beta\big(\eta\nu_1(\rho),\eta\big)\eta+g\big(\eta+\eta\nu_1(\rho)\big)\eta\leq\lambda_A(\rho)\eta,$$

which is $\mathbf{F}_2(\eta\nu_1(\rho),\eta)\leq\eta\big(\mathbf{F}'_{21}(0,0),\mathbf{F}'_{22}(0,0)\big)\cdot(\eta\nu_1(\rho),\eta)^T$.

Therefore, if (4) satisfies (41)–(42), (46)–(47), and (52)–(53), then (4) also satisfies (66)–(70). □

Since the general go-or-grow model (4) satisfies the general conditions (66)–(70), we can apply the following lemma to obtain information on the spreading speed.

Lemma 10 *(Liang and Zhao 2007; Fang and Zhao 2009; Weinberger et al. 2002) Let* $\mathbf{F}$ *satisfy* (66)–(68)*, and consider the initial condition* $\phi \in \mathcal{C}_{\bar{\mathbf{w}}} = \{(\phi_1, \ldots, \phi_n) \in C(\mathbb{R}; \mathbb{R}^n) : 0 \leq \phi_i(z) \leq \bar{w}_i \ \forall z \in \mathbb{R}\}$ *and* $\mathbf{w}(t, x; \phi)$ *be the unique solution of* (65) *through* ϕ*. Then there exists a real number* $0 < \tilde{c} \leq \bar{c}$*, where*

$$\bar{c} = \inf_{\rho > 0} \Phi(\rho), \tag{72}$$

such that the following statements are valid:

- *(i)* $\Phi(\rho) = \dfrac{\lambda_A(\rho)}{\rho}$ *is decreasing as* ρ *nears 0 and tends to infinity as* $\rho \to 0$*;* $\Phi'(\rho)$ *changes sign at most once in* $(0, \infty)$ *and* $\lim_{\rho \to \infty} \Phi(\rho) = +\infty$*;*
- *(ii) If* ϕ *has compact support, then* $\lim_{\substack{t \to \infty \\ |x| \geq ct}} \mathbf{w}(t, x; \phi) = 0$*, for all* $c > \tilde{c}$*;*
- *(iii) For any* $c \in (0, \tilde{c})$ *and any vector* $\mathbf{r} > \mathbf{0}$*, there is a positive number* $R_{\mathbf{r}}$ *such that for any* $\phi \in \mathcal{C}_{\bar{\mathbf{w}}}$ *with* $\phi \leq \mathbf{r}$ *on an interval of length* $2R_{\mathbf{r}}$*, it holds that*

$$\lim_{\substack{t \to \infty \\ |x| \leq ct}} \mathbf{w}(t, x; \phi) = \bar{\mathbf{w}};$$

- *(iv) If, in addition,* $\mathbf{F}(\min\{\eta \boldsymbol{\nu}(\rho^*), \mathbf{1}\}) \leq \eta \mathbf{F}'(\mathbf{0}) \boldsymbol{\nu}(\rho)$, for all $\eta > 0$*, then* $\tilde{c} = \bar{c}$*, where* ρ^* *is the value of* ρ *at which* $\Phi(\rho)$ *attains its infimum.*

Finally, we use the following theorem to prove the existence of traveling wave solutions.

Theorem 11 *(Theorem 3.1 in Fang and Zhao (2009)) Assume the set of assumptions (66)–(70) hold, then for each* $c \geq \bar{c}$*, system (65) has a non increasing wave front* $W(x - ct)$ *connecting* $\mathbf{0}$ *and* $\bar{\mathbf{w}}$*; while for any* $c \in (0, \bar{c})$*, there is no wavefront* $W(x - ct)$ *connecting* $\mathbf{0}$ *and* $\bar{\mathbf{w}}$*.*

Applying Lemma 10 and Theorem 11 to the general go-or-grow model (4), with assumptions, (41)–(42), (46)–(47), and (52)–(53), proves Lemma 6 and Theorem 7.

Acknowledgements We are grateful to the Fields Institute in Toronto, who hosted us for a few weeks in Summer and Fall 2024 to work on this project. RT acknowledges support from a Canadian Graduate Scholarship of the Natural Sciences and Engineering Research Council of Canada (NSERC) and Alberta

Innovates Graduate Student Scholarship. MC was supported by the National Group of Mathematical Physics (GNFM-INdAM) through the INdAM-GNFM Project (CUP E53C22001930001) "From kinetic to macroscopic models for tumor-immune system competition", and by the European Union - NextGenerationEU and the MUR-Italian Ministry of Universities and Research through the project PRIN 2022 PNRR *Mathematical modeling for a Sustainable Circular Economy in Ecosystems* (project code P2022PSMT7, CUP D53D23018960001). TLS acknowledges support from a National Science Foundation (NSF) grant DMS-2151566. TH is supported through a discovery grant of the Natural Science and Engineering Research Council of Canada (NSERC), RGPIN-2023-04269.

Data availability Data sharing is not applicable to this article as no data sets were generated or analyzed during the current study.

Declarations

Conflict of interest We declare that TH is currently an Editor-in-Chief of the Journal of Mathematical Biology. The research was conducted in the absence of any commercial or financial interests that could be construed as a potential Conflict of interest.

Open Access This article is licensed under a Creative Commons Attribution-NonCommercial-NoDerivatives 4.0 International License, which permits any non-commercial use, sharing, distribution and reproduction in any medium or format, as long as you give appropriate credit to the original author(s) and the source, provide a link to the Creative Commons licence, and indicate if you modified the licensed material. You do not have permission under this licence to share adapted material derived from this article or parts of it. The images or other third party material in this article are included in the article's Creative Commons licence, unless indicated otherwise in a credit line to the material. If material is not included in the article's Creative Commons licence and your intended use is not permitted by statutory regulation or exceeds the permitted use, you will need to obtain permission directly from the copyright holder. To view a copy of this licence, visit http://creativecommons.org/licenses/by-nc-nd/4.0/.

References

Alfonso J et al (2017) The biology and mathematical modelling of glioma invasion: a review. J R Soc Interface 14:20170490. https://doi.org/10.1098/rsif.2017.0490

Alfonso JCL et al (2016) Why one-size-fits-all vaso-modulatory interventions fail to control glioma invasion: in silico insights. Sci Rep 6:37283. https://doi.org/10.1038/srep37283

Alsisi A, Eftimie R, Trucu D (2021) Non-local multiscale approach for the impact of go or grow hypothesis on tumour-viruses interactions. Math Biosci Eng 18:5252–5284. https://doi.org/10.3934/mbe.2021267

Ayuso JM et al (2017) Glioblastoma on a microfluidic chip: Generating pseudopalisades and enhancing aggressiveness through blood vessel obstruction events. Neuro Oncol 19:503–513. https://doi.org/10.1093/neuonc/now230

Berens M.E, Giese A (1999).... those left behind." Biology and oncology of invasive glioma cells. Neoplasia 1:208–219. https://doi.org/10.1038/sj.neo.7900034

Billingham J, Needham DJ (1991) The development of travelling waves in quadratic and cubic autocatalysis with unequal diffusion rates. I. Permanent form travelling waves. Philosophical Transactions of the Royal Society of London. Series A: Physical and Engineering Sciences 334:1–24. https://doi.org/10.1098/rsta.1991.0001

Böttger K, Hatzikirou H, Chauviere A, Deutsch A (2012) Investigation of the migration/proliferation dichotomy and its impact on avascular glioma invasion. Math Modelling Nat Phenomena 7:105–135. https://doi.org/10.1051/mmnp/20127106

Böttger K et al (2015) An emerging Allee effect is critical for tumor initiation and persistence. PLoS Comput Biol 11:e1004366. https://doi.org/10.1371/journal.pcbi.1004366

Britton N (1986) Reaction-Diffusion Equations and Their Applications to Biology. Academic Press, London

Burger M, Friele P, Pietschmann J-F (2020) On a reaction-cross-diffusion system modeling the growth of glioblastoma. SIAM J Appl Math 80:160–182. https://doi.org/10.1137/18M1194559
Canosa J (1973) On a nonlinear diffusion equation describing population growth. IBM J Res Dev 17:307–313. https://doi.org/10.1147/rd.174.0307
Capasso V, Maddalena L (1981) Convergence to equilibrium states for a reaction-diffusion system modelling the spatial spread of a class of bacterial and viral diseases. J Math Biol 13:173–184. https://doi.org/10.1007/BF00275212
Chauviere A, Preziosi L, Byrne H (2010) A model of cell migration within the extracellular matrix based on a phenotypic switching mechanism. Math Med Biol 27:255–281. https://doi.org/10.1093/imammb/dqp021
Chen C, Wang H (2024) Steady-state bifurcation and spike pattern in the Klausmeier-Gray-Scott model with non-diffusive plants. Discrete Contin Dyn Syst B 29:4973–4999. https://doi.org/10.3934/dcdsb.2024074
Chuan LH, Tsujikawa T, Yagi A (2006) Asymptotic behavior of solutions for forest kinematic model. Funkcialaj Ekvacioj 49:427–449. https://doi.org/10.1619/fesi.49.427
Ciocanel M-V, Sandstede B, Jeschonek SP, Mowry KL (2018) Modeling microtubule-based transport and anchoring of mRNA. SIAM J Appl Dyn Syst 17:2855–2881. https://doi.org/10.1137/18M1186083
Cochet-Escartin O et al (2021) Hypoxia triggers collective aerotactic migration in Dictyostelium discoideum. Elife 10:e64731. https://doi.org/10.7554/eLife.64731
Colombo MC et al (2015) Towards the personalized treatment of glioblastoma: Integrating patient-specific clinical data in a continuous mechanical model. PLoS One 10:e0132887. https://doi.org/10.1371/journal.pone.0132887
Conte M, Gerardo-Giorda L, Groppi M (2020) Glioma invasion and its interplay with nervous tissue and therapy: A multiscale model. J Theor Biol 486:110088. https://doi.org/10.1016/j.jtbi.2019.110088
Conte M, Casas-Tinto S, Soler J (2021) Modeling invasion patterns in the glioblastoma battlefield. PLoS Comput Biol 17:e1008632. https://doi.org/10.1371/journal.pcbi.1008632
Conte M, Dzierma Y, Knobe S, Surulescu C (2023) Mathematical modeling of glioma invasion and therapy approaches via kinetic theory of active particles. Math Models Methods Appl Sci 33:1009–1051. https://doi.org/10.1142/S0218202523500227
Conte M, Surulescu C (2021) Mathematical modeling of glioma invasion: Acid- and vasculature mediated go-or-grow dichotomy and the influence of tissue anisotropy. Appl Math Comput 407:126305. https://doi.org/10.1016/j.amc.2021.126305
Crossley RM, Painter KJ, Lorenzi T, Maini PK, Baker RE (2024) Phenotypic switching mechanisms determine the structure of cell migration into extracellular matrix under the 'go-or-grow' hypothesis. Math Biosci 374:109240. https://doi.org/10.1016/j.mbs.2024.109240
Cuddapah VA, Robel S, Watkins S, Sontheimer H (2014) A neurocentric perspective on glioma invasion. Nat Rev Neurosci 15:455–465. https://doi.org/10.1038/nrn3765
Curtin L, Hawkins-Daarud A, Van Der Zee KG, Swanson KR, Owen MR (2020) Speed switch in glioblastoma growth rate due to enhanced hypoxia-induced migration. Bull Math Biol 82:43. https://doi.org/10.1007/s11538-020-00718-x
Curtin L et al (2020) A mechanistic investigation into ischemia-driven distal recurrence of glioblastoma. Bull Math Biol 82:143. https://doi.org/10.1007/s11538-020-00814-y
de Vries G, Hillen T, Lewis M, Müller J, Schönfisch B (2006) A course in mathematical biology: quantitative modeling with mathematical and computational methods. SIAM, Philadelphia
Dunbar SR (1984) Traveling wave solutions of diffusive Lotka-Volterra equations: A heteroclinic connection in [CDATA[R^4]]R^4. Trans Am Math Soc 286:557–594. https://doi.org/10.2307/1999810
Dunbar SR (1986) Traveling waves in diffusive predator-prey equations: Periodic orbits and point-to-periodic heteroclinic orbits. SIAM J Appl Math 46:1057–1078. https://doi.org/10.1137/0146063
Dunbar SR (1983) Travelling wave solutions of diffusive Lotka-Volterra equations. J Math Biol 17:11–32. https://doi.org/10.1007/BF00276112
Engwer C, Hillen T, Knappitsch M, Surulescu C (2015) Glioma follow white matter tracts: a multiscale DTI-based model. J Math Biol 71:551–582. https://doi.org/10.1007/s00285-014-0822-7
Engwer C, Hunt A, Surulescu C (2016) Effective equations for anisotropic glioma spread with proliferation: A multiscale approach and comparisons with previous settings. Math Med Biol J IMA 33:435–459. https://doi.org/10.1093/imammb/dqv030
Engwer C, Knappitsch M, Surulescu C (2015) A multiscale model for glioma spread including cell-tissue interactions and proliferation. Math Biosci Eng 13:443–460. https://doi.org/10.3934/mbe.2015011

Falcó C, Crossley RM, Baker RE (2024) Travelling waves in a minimal go-or-grow model of cell invasion. Appl Math Lett 158:109209. https://doi.org/10.1016/j.aml.2024.109209
Fang J, Zhao X-Q (2009) Monotone wavefronts for partially degenerate reaction-diffusion systems. J Dyn Diff Equat 21:663–680. https://doi.org/10.1007/s10884-009-9152-7
Farin A et al (2006) Transplanted glioma cells migrate and proliferate on host brain vasculature: A dynamic analysis. Glia 53:799–808. https://doi.org/10.1002/glia.20334
Fedotov S, Iomin A (2008) Probabilistic approach to a proliferation and migration dichotomy in tumor cell invasion. Phys Rev E 77:031911. https://doi.org/10.1103/PhysRevE.77.031911
Fedotov S, Iomin A (2007) Migration and proliferation dichotomy in tumor-cell invasion. Phys Rev Lett 98:118101. https://doi.org/10.1103/PhysRevLett.98.118101
Finlayson A, Merkin J (1997) Travelling waves in an open quadratic autocatalytic chemical system. J Math Chem 21:305–321. https://doi.org/10.1023/A:1019134822110
Garay T et al (2013) Cell migration or cytokinesis and proliferation? - Revisiting the "go or grow" hypothesis in cancer cells in vitro. Exp Cell Res 319:3094–3103. https://doi.org/10.1016/j.yexcr.2013.08.018
Gerlee P, Nelander S (2012) The impact of phenotypic switching on glioblastoma growth and invasion. PLoS Comput Biol 8:e1002556. https://doi.org/10.1371/journal.pcbi.1002556
Gerlee P, Nelander S (2016) Travelling wave analysis of a mathematical model of glioblastoma growth. Math Biosci 276:75–81. https://doi.org/10.1016/j.mbs.2016.03.004
Giese A, Bjerkvig R, Berens M, Westphal M (2003) Cost of migration: Invasion of malignant gliomas and implications for treatment. J Clin Oncol 21:1624–1636. https://doi.org/10.1200/JCO.2003.05.063
Giese A et al (1996) Dichotomy of astrocytoma migration and proliferation. Int J Cancer 67:275–282. https://doi.org/10.1002/(SICI)1097-0215(19960717)67:2275::AID-IJC203.0.CO;2-9
Godlewski J, Bronisz A, Nowicki MO, Chiocca EA, Lawler S (2010) microRNA-451: A conditional switch controlling glioma cell proliferation and migration. Cell Cycle 9:2814–2820. https://doi.org/10.4161/cc.9.14.12248
Hadeler K, Lewis M (2002) Spatial dynamics of the diffusive logistic equation with a sedentary compartment. Can Appl Math Q 10:473–498
Härting S, Marciniak-Czochra A (2014) Spike patterns in a reaction-diffusion ODE model with Turing instability. Math Methods Appl Sci 37:1377–1391. https://doi.org/10.1002/mma.2899
Hatzikirou H, Basanta D, Simon M, Schaller K, Deutsch A (2012) "Go or grow": The key to the emergence of invasion in tumour progression? Mathematical Medicine and Biology: A Journal of the IMA 29:49–65. https://doi.org/10.1093/imammb/dqq011
Hatzikirou H, Deutsch A, Schaller C, Simon M, Swanson K (2005) Mathematical modelling of glioblastoma tumour development: A review. Math Models Methods Appl Sci 15:1779–1794. https://doi.org/10.1142/S0218202505000960
Hillen T (2023) Elements of Applied Functional Analysis. American Mathematical Society Open Math Notes, Providence, RI
Hillen T, Loy N, Painter K, Thiessen R (2024) Modelling microtube driven invasion of glioma. J Math Biol 88:1–34. https://doi.org/10.1007/s00285-023-02025-0
Hoek KS et al (2008) In vivo switching of human melanoma cells between proliferative and invasive states. Can Res 68:650–656. https://doi.org/10.1158/0008-5472.CAN-07-2491
Hormuth D et al (2022) Opportunities for improving brain cancer treatment outcomes through imaging-based mathematical modeling of the delivery of radiotherapy and immunotherapy. Adv Drug Deliv Rev 187:114367. https://doi.org/10.1016/j.addr.2022.114367
Hou LC, Veeravagu A, Hsu AR, Victor C (2006) Recurrent glioblastoma multiforme: A review of natural history and management options. Neurosurg Focus 20:E3. https://doi.org/10.3171/foc.2006.20.4.2
Hsu C-H, Yang C-R, Yang T-H, Yang T-S (2012) Existence of traveling wave solutions for diffusive predator-prey type systems. J Differential Equations 252:3040–3075. https://doi.org/10.1016/j.jde.2011.11.008
Huang J, Lu G, Ruan S (2003) Existence of traveling wave solutions in a diffusive predator-prey model. J Math Biol 46:132–152. https://doi.org/10.1007/s00285-002-0171-9
Huang Q, Jin Y, Lewis MA (2016) R_0[CDATA[R_0]] analysis of a benthic-drift model for a stream population. SIAM J Appl Dyn Syst 15:287–321. https://doi.org/10.1137/15M1014486
Huang Q, Wang H, Lewis MA (2017) A hybrid continuous/discrete-time model for invasion dynamics of zebra mussels in rivers. SIAM J Appl Math 77:854–880. https://doi.org/10.1137/16M1057826
Huang W (2016) A geometric approach in the study of traveling waves for some classes of non-monotone reaction-diffusion systems. J Differential Equations 260:2190–2224. https://doi.org/10.1016/j.jde.2015.09.060

Huang W (2012) Traveling wave solutions for a class of predator-prey systems. J Dyn Diff Equat 24:633–644. https://doi.org/10.1007/s10884-012-9255-4
Hunt A, Surulescu C (2017) A multiscale modeling approach to glioma invasion with therapy. Vietnam J Math 45:221–240. https://doi.org/10.1007/s10013-016-0223-x
Jbabdi S et al (2005) Simulation of anisotropic growth of low-grade gliomas using diffusion tensor imaging. Magn Reson Med 54:616–624. https://doi.org/10.1002/mrm.20625
Jin Y, Zhao X-Q (2021) The spatial dynamics of a zebra mussel model in river environments. Discrete Contin Dyn Syst B 26:1991–2010. https://doi.org/10.3934/dcdsb.2020362
Jørgensen ACS et al (2023) Data-driven spatio-temporal modelling of glioblastoma. Royal Soc Open Sci 10:221444. https://doi.org/10.1098/rsos.221444
Kim Y, Lawler S, Nowicki MO, Chiocca EA, Friedman A (2009) A mathematical model for pattern formation of glioma cells outside the tumor spheroid core. J Theor Biol 260:359–371. https://doi.org/10.1016/j.jtbi.2009.06.025
Kim Y, Roh S (2013) A hybrid model for cell proliferation and migration in glioblastoma. Discrete Contin Dyn Syst-B 18:969–1015. https://doi.org/10.3934/dcdsb.2013.18.969
Kuznetsov M, Kolobov A (2020) Investigation of solid tumor progression with account of proliferation/migration dichotomy via Darwinian mathematical model. J Math Biol 80:601–626. https://doi.org/10.1007/s00285-019-01434-4
Kuznetsov YA, Antonovsky MY, Biktashev VN, Aponina EA (1994) A cross-diffusion model of forest boundary dynamics. J Math Biol 32:219–232. https://doi.org/10.1007/BF00163879
Lam K-Y, Wang X, Zhang T (2018) Traveling waves for a class of diffusive disease-transmission models with network structures. SIAM J Math Anal 50:5719–5748. https://doi.org/10.1137/17M114425
Landman KA, Cai AQ, Hughes BD (2007) Travelling waves of attached and detached cells in a wound-healing cell migration assay. Bull Math Biol 69:2119–2138. https://doi.org/10.1007/s11538-007-9206-0
Levin S, Okubo A (2002) *Diffusion and Ecological Problems: Modern Perspectives* 2nd. https://doi.org/10.1007/978-1-4757-4978-6 (Springer-Verlag, New York)
Lewis MA, Schmitz G, Kareiva P, Trevors JT (1996) Models to examine containment and spread of genetically engineered microbes. Mol Ecol 5:165–175. https://doi.org/10.1046/j.1365-294X.1996.00228.x
Lewis M, Li B, Weinberger H (2002) Spreading Speed and Linear Determinancy for two-species competition model. J Math Biol 45:219–312. https://doi.org/10.1007/s002850200144
Lewis M, Schmitz G (1996) Biological invasion of an organism with separate mobile and stationary states: Modeling and analysis. Forma 11:1–25
Li W-T, Wu S-L (2008) Traveling waves in a diffusive predator-prey model with Holling type-III functional response. Chaos Solitons Fractals 37:476–486. https://doi.org/10.1016/j.chaos.2006.09.039
Liang X, Zhang L, Zhao X-Q (2017) The principal eigenvalue for degenerate periodic reaction-diffusion systems. SIAM J Math Anal 49:3603–3636. https://doi.org/10.1137/16M1108832
Liang X, Zhao X-Q (2007) Asymptotic speeds of spread and traveling waves for monotone semiflows with applications. Commun Pure Appl Math 60:1–40. https://doi.org/10.1002/cpa.20154
Lin X, Weng P, Wu C (2011) Traveling wave solutions for a predator-prey system with sigmoidal response function. J Dyn Diff Equat 23:903–921. https://doi.org/10.1007/s10884-011-9220-7
Lutscher F, Lewis MA, McCauley E (2006) Effects of heterogeneity on spread and persistence in rivers. Bull Math Biol 68:2129–2160. https://doi.org/10.1007/s11538-006-9100-1
Lutscher F, McCauley E, Lewis MA (2007) Spatial patterns and coexistence mechanisms in systems with unidirectional flow. Theor Popul Biol 71:267–277. https://doi.org/10.1016/j.tpb.2006.11.006
Lutscher F, Seo G (2011) The effect of temporal variability on persistence conditions in rivers. J Theor Biol 283:53–59. https://doi.org/10.1016/j.jtbi.2011.05.032
Marciniak-Czochra A *Reaction-diffusion-ODE models of pattern formation* in *Evolutionary Equations with Applications in Natural Sciences* (eds Banasiak, J. & Mokhtar-Kharroubi, M.) 387–438 (Springer International Publishing, Cham, 2015). https://doi.org/10.1007/978-3-319-11322-7_8
Martirosyan NL et al (2015) Mathematically modeling the biological properties of gliomas: A review. Math Biosci Eng 12:879–905. https://doi.org/10.3934/mbe.2015.12.879
Martınez-González A, Calvo G.F., Pérez Romasanta L.A., Pérez-Garcıa V.M. (2012) Hypoxic cell waves around necrotic cores in glioblastoma: a biomathematical model and its therapeutic implications. Bull Math Biol 74:2875–2896. https://doi.org/10.1007/s11538-012-9786-1
Merkin J, Sadiq MA (1996) The propagation of travelling waves in an open cubic autocatalytic chemical system. IMA J Appl Math 57:273–309. https://doi.org/10.1093/imamat/57.3.273
Merkin JH, Petrov V, Scott SK, Showalter K (1996) Wave-induced chemical chaos. Phys Rev Lett 76:546–549. https://doi.org/10.1103/PhysRevLett.76.546

Murray JD (2002). Mathematical Biology: I An Introduction. https://doi.org/10.1007/b98868 (Springer, New York, NY)
Murray JD (2003) Mathematical Biology: II. Spatial Models and Biomedical Applications. https://doi.org/10.1007/b98869 (Springer, New York, NY)
Odde DJ (2023) Glioblastoma cell invasion: Go? Grow? Yes. https://doi.org/10.1093/neuonc/noad178
Osswald M et al (2015) Brain tumour cells interconnect to a functional and resistant network. Nature 528:93–98. https://doi.org/10.1038/nature16071
Ostrom QT et al (2014) The epidemiology of glioma in adults: a "state of the science" ' review. Neuro Oncol 16:896–913. https://doi.org/10.1093/neuonc/nou087
Pachepsky E, Lutscher F, Nisbet R, Lewis M (2005) Persistence, spread and the drift paradox. Theor Popul Biol 67:61–73. https://doi.org/10.1016/j.tpb.2004.09.001
Painter K, Hillen T (2013) Mathematical modelling of glioma growth: the use of diffusion tensor imaging (DTI) data to predict the anisotropic pathways of cancer invasion. J Theor Biol 323:25–39. https://doi.org/10.1016/j.jtbi.2013.01.014
Pardo R, Martınez-González A, Pérez-Garcıa VM (2016) Nonlinear ghost waves accelerate the progression of high-grade brain tumors. Commun Nonlinear Sci Numer Simul 39:360–380. https://doi.org/10.1016/j.cnsns.2016.03.014
Patra P, Klumpp S (2021) Role of bacterial persistence in spatial population expansion. Phys Rev E 104:034401. https://doi.org/10.1103/PhysRevE.104.034401
Perko L (2013) Differential equations and dynamical systems. Springer Science & Business Media, Berlin
Pham K et al (2012) Density-dependent quiescence in glioma invasion: instability in a simple reaction-diffusion model for the migration/proliferation dichotomy. J Biol Dyn 6:54–71. https://doi.org/10.1080/17513758.2011.590610
Quinn T, Sinkala Z (2009) Dynamics of prostate cancer stem cells with diffusion and organism response. Biosystems 96:69–79. https://doi.org/10.1016/j.biosystems.2008.11.010
Ratliff M et al (2023) Individual glioblastoma cells harbor both proliferative and invasive capabilities during tumor progression. Neuro Oncol 25:2150–2162. https://doi.org/10.1093/neuonc/noad109
Robinson J (2001) Infinite-Dimensional Dynamical Systems. Cambridge University Press, Cambridge
Rothe F (1984) Global solutions of reaction-diffusion systems. Springer, Berlin
Sadiq MA, Merkin JH (1996) Travelling waves in an open cubic autocatalytic system. J Math Chem 20:213–233. https://doi.org/10.1007/BF01165344
Saut O, Lagaert J-B, Colin T, Fathallah-Shaykh HM (2014) A multilayer grow-or-go model for GBM: Effects of invasive cells and anti-angiogenesis on growth. Bull Math Biol 76:2306–2333. https://doi.org/10.1007/s11538-014-0007-y
Scribner E, Fathallah-Shaykh HM (2017) Single cell mathematical model successfully replicates key features of GBM: go-or-grow is not necessary. PLoS One 12:e0169434. https://doi.org/10.1371/journal.pone.0169434
Sewalt L, Doelman A (2017) Spatially periodic multipulse patterns in a generalized Klausmeier-Gray-Scott model. SIAM J Appl Dyn Syst 16:1113–1163. https://doi.org/10.1137/16M1078756
Sherratt Jonathan A. (2000) Wavefront propagation in a competition equation with a new motility term modelling contact inhibition between cell populations. In: Proceedings of the Royal Society of London. Series A: Mathematical, Physical and Engineering Sciences 456(2002):2365–2386. https://doi.org/10.1098/rspa.2000.0616
Sherratt JA, Chaplain MA (2001) A new mathematical model for avascular tumour growth. J Math Biol 43:291–312. https://doi.org/10.1007/s002850100088
Smoller J (1983) Shock waves and reaction-diffusion equations. Springer-Verlag, New York. https://doi.org/10.1007/978-1-4612-0873-0
Stein AM, Demuth T, Mobley D, Berens M, Sander LM (2007) A mathematical model of glioblastoma tumor spheroid invasion in a three-dimensional in vitro experiment. Biophys J 92:356–365. https://doi.org/10.1529/biophysj.106.093468
Stein S, Zhao R, Haeno H, Vivanco I, Michor F (2018) Mathematical modeling identifies optimum lapatinib dosing schedules for the treatment of glioblastoma patients. PLoS Comput Biol 14:e1005924. https://doi.org/10.1371/journal.pcbi.1005924
Stepien TL, Rutter EM, Kuang Y (2018) Traveling waves of a go-or-grow model of glioma growth. SIAM J Appl Math 78:1778–1801. https://doi.org/10.1137/17M1146257
Stinner C, Surulescu C, Uatay A (2016) Global existence for a go-or-grow multiscale model for tumor invasion with therapy. Math Models Methods Appl Sci 26:2163–2201. https://doi.org/10.1142/S0218202516400011X

Swan A, Hillen T, Bowman JC, Murtha AD (2018) A patient-specific anisotropic diffusion model for brain tumour spread. Bull Math Biol 80:1259–1291. https://doi.org/10.1007/s11538-017-0271-8

Swanson K, Rostomily R, Alvord E (2008) A mathematical modelling tool for predicting survival of individual patients following resection of glioblastoma: A proof of principle. Br J Cancer 98:113–119. https://doi.org/10.1038/sj.bjc.6604125

Swanson K, Bridge C, Murray J Jr (2003) Virtual and real brain tumors: Using mathematical modeling to quantify glioma growth and invasion. J Neurol Sci 216:1–10. https://doi.org/10.1016/j.jns.2003.06.001

Swanson KR et al (2011) Quantifying the role of angiogenesis in malignant progression of gliomas: in silico modeling integrates imaging and histology. Can Res 71:7366–7375. https://doi.org/10.1158/0008-5472.CAN-11-1399

Syga S, Jain HP, Krellner M, Hatzikirou H, Deutsch A (2024) Evolution of phenotypic plasticity leads to tumor heterogeneity with implications for therapy. PLoS Comput Biol 20:1–18. https://doi.org/10.1371/journal.pcbi.1012003

Tektonidis M et al (2011) Identification of intrinsic in vitro cellular mechanisms for glioma invasion. J Theor Biol 287:131–147. https://doi.org/10.1016/j.jtbi.2011.07.012

Thiessen R, Hillen T (2021) Anisotropic network patterns in kinetic and diffusive chemotaxis models. Mathematics 9:1561. https://doi.org/10.3390/math9131561

Turing, A.M. The chemical basis of morphogenesis. *Philosophical Transactions of the Royal Society of London. Series B, Biological Sciences***237,** 37–72. https://doi.org/10.1098/rstb.1952.0012 (1952)

Tursynkozha A, Kashkynbayev A, Shupeyeva B, Rutter EM, Kuang Y (2023) Traveling wave speed and profile of a "or grow" glioblastoma multiforme model. Commun Nonlinear Sci Numer Simul 118:107008. https://doi.org/10.1016/j.cnsns.2022.107008

Van der Stelt S, Doelman A, Hek G, Rademacher JDM (2013) Rise and fall of periodic patterns for a generalized Klausmeier-Gray-Scott model. J Nonlinear Sci 23:39–95. https://doi.org/10.1007/s00332-012-9139-0

Venegas-Ortiz J, Allen RJ, Evans MR (2014) Speed of invasion of an expanding population by a horizontally transmitted trait. Genetics 196:497–507. https://doi.org/10.1534/genetics.113.158642

Vittadello ST, McCue SW, Gunasingh G, Haass NK, Simpson MJ (2020) Examining go-or-grow using fluorescent cell-cycle indicators and cell-cycle-inhibiting drugs. Biophys J 118:1243–1247. https://doi.org/10.1016/j.bpj.2020.01.036

Wang M (2024) Pang PY Upper and lower solutions method for single equations. Nonlinear Second Order Elliptic Equations. https://doi.org/10.1007/978-981-99-8692-7_3

Wang SD et al (2012) EphB2 receptor controls proliferation/migration dichotomy of glioblastoma by interacting with focal adhesion kinase. Oncogene 31:5132–5143. https://doi.org/10.1038/onc.2012.16

Wang Y, Shi J (2020) Analysis of a reaction-diffusion benthic-drift model with strong Allee effect growth. J Differential Equations 269:7605–7642. https://doi.org/10.1016/j.jde.2020.05.044

Weinberger HF, Lewis MA, Li B (2002) Analysis of linear determinacy for spread in cooperative models. J Math Biol 45:183–218. https://doi.org/10.1007/s002850200145

Wick W, Osswald M, Wick A, Winkler F (2018) Treatment of glioblastoma in adults. Ther Adv Neurol Disord 11:1756286418790452. https://doi.org/10.1177/1756286418790452

Xie Q, Mittal S, Berens ME (2014) Targeting adaptive glioblastoma: An overview of proliferation and invasion. Neuro Oncol 16:1575–1584. https://doi.org/10.1093/neuonc/nou147

Xin J (2000) Front propagation in heterogeneous media. SIAM Rev. https://doi.org/10.1137/S00361445 9936429

Yan X, Nie H, Zhou P (2022) On a competition-diffusion-advection system from river ecology: Mathematical analysis and numerical study. SIAM J Appl Dyn Syst 21:438–469. https://doi.org/10.1137/20M1387924

Zhang T (2017) Minimal wave speed for a class of non-cooperative reaction-diffusion systems of three equations. J Differential Equations 262:4724–4770. https://doi.org/10.1016/j.jde.2016.12.017

Zhang T, Wang W (2014) Existence of traveling wave solutions for influenza model with treatment. J Math Anal Appl 419:469–495. https://doi.org/10.1016/j.jmaa.2014.04.068

Zhang T, Wang W, Wang K (2016) Minimal wave speed for a class of non-cooperative diffusion-reaction system. J Differential Equations 260:2763–2791. https://doi.org/10.1016/j.jde.2015.10.017

Zhao X-Q, Zhou P (2016) On a Lotka-Volterra competition model: The effects of advection and spatial variation. Calc Var Partial Differ Equ 55:73. https://doi.org/10.1007/s00526-016-1021-8

Zhigun A, Surulescu C, Hunt A (2018) A strongly degenerate diffusion-haptotaxis model of tumour invasion under the go-or-grow dichotomy hypothesis. Math Methods Appl Sci 41:2403–2428. https://doi.org/10.1002/mma.4749

Zhu H, Ou C (2011) Existence of traveling wavefronts for Sherratt's avascular tumor model. Chaos Solitons Fractals 44:218–225. https://doi.org/10.1016/j.chaos.2011.01.011

Zhu H, Yuan W, Ou C (2008) Justification for wavefront propagation in a tumour growth model with contact inhibition. In: Proceedings of the Royal Society A: Mathematical, Physical and Engineering Sciences 464:1257–1273. https://doi.org/10.1098/rspa.2007.0097

Publisher's Note Springer Nature remains neutral with regard to jurisdictional claims in published maps and institutional affiliations.